Electronic Supplementary Information

Synthesis and Characterization of Photoluminescence Liquid Crystals Based on Flexible Chain-Bearing Pentafluorinated Bistolanes

Shigeyuki Yamada *, Masaya Sato and Tsutomu Konno

Faculty of Molecular Chemistry and Engineering, Kyoto Institute of Technology, Matsugasaki, Sakyo-ku, Kyoto 606-8585, Japan; kit.fusso.201803@gmail.com (M.S.); konno@kit.ac.jp (T.K.)
* Correspondence: syamada@kit.ac.jp; Tel.: +81-75-724-7517

Table of contents

1. NMR Spectra

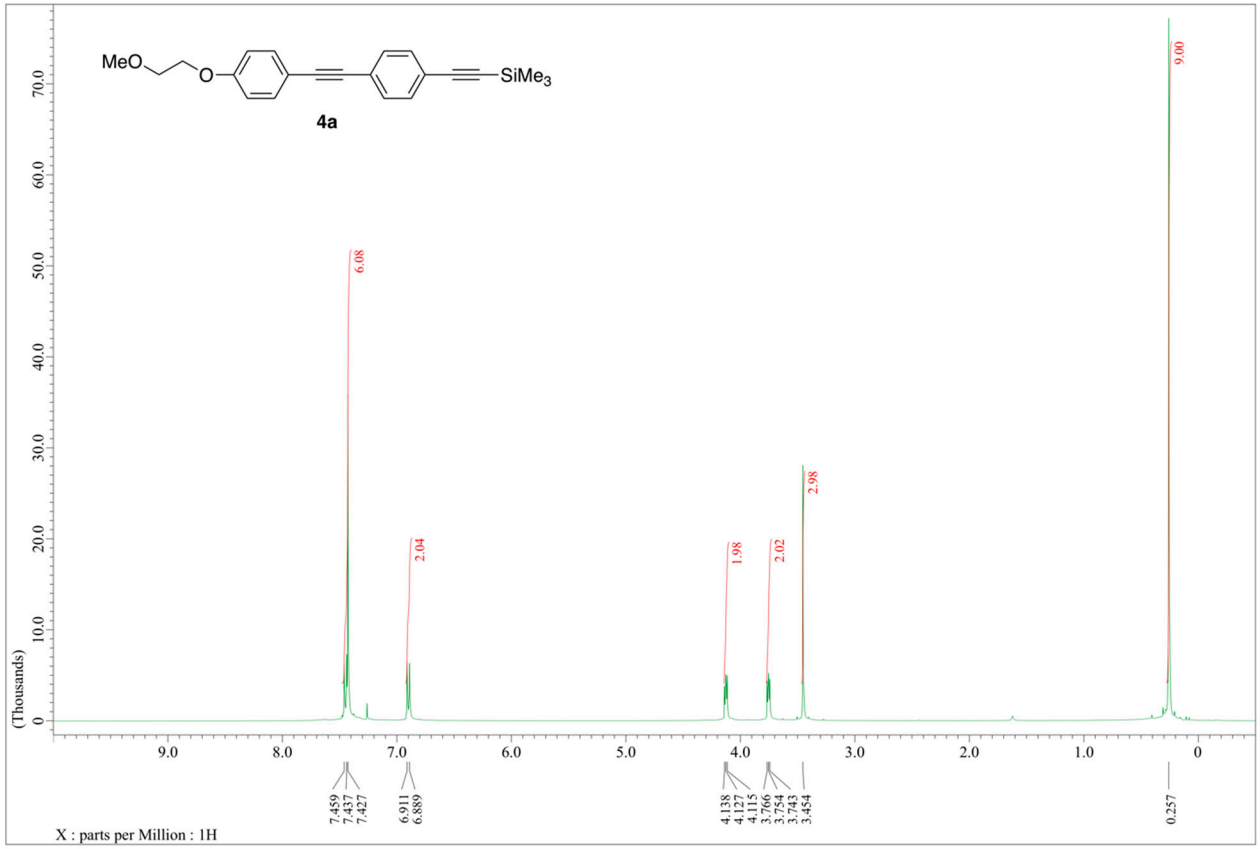

Figure S1. ^{1}H NMR spectrum of **4a** (Solvent: $CDCl_3$)

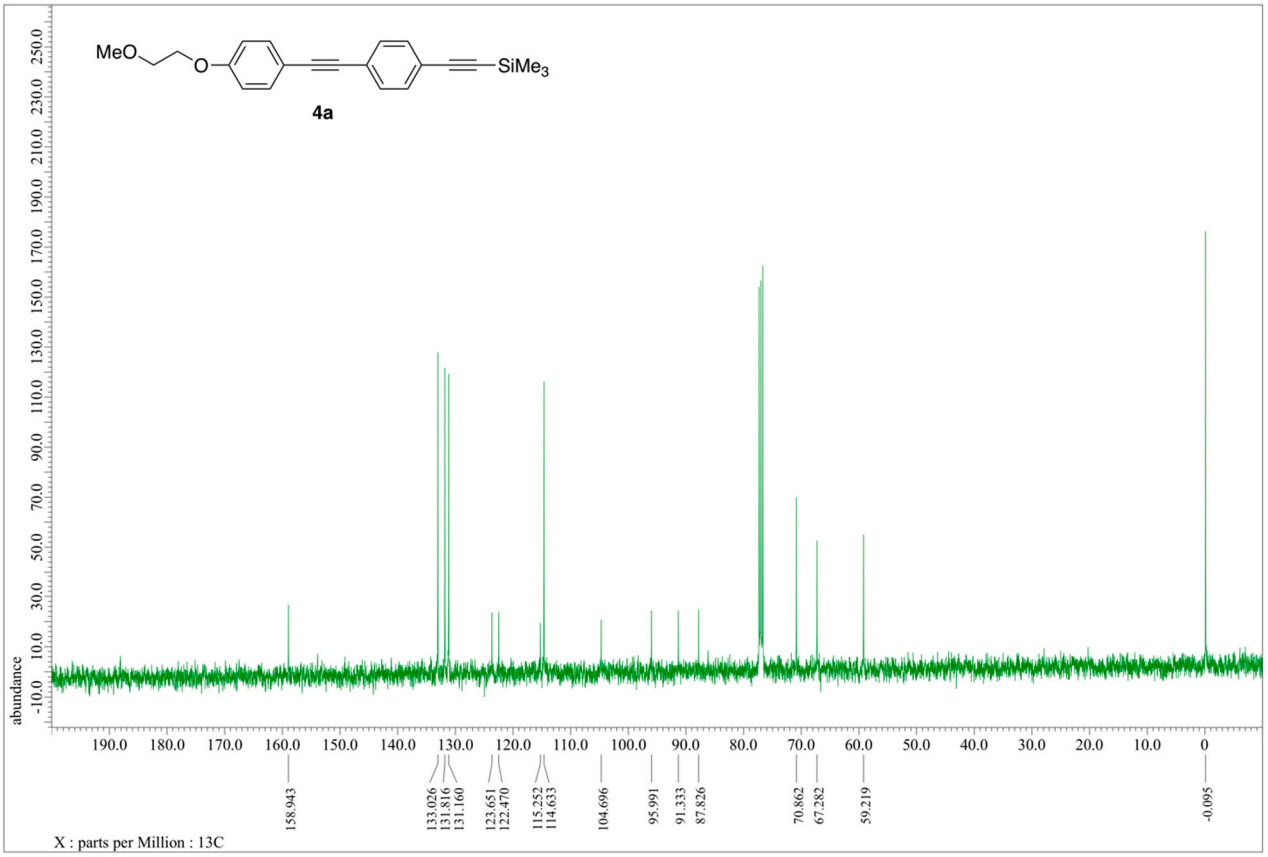

Figure S2. ^{13}C NMR spectrum of **4a** (Solvent: $CDCl_3$)

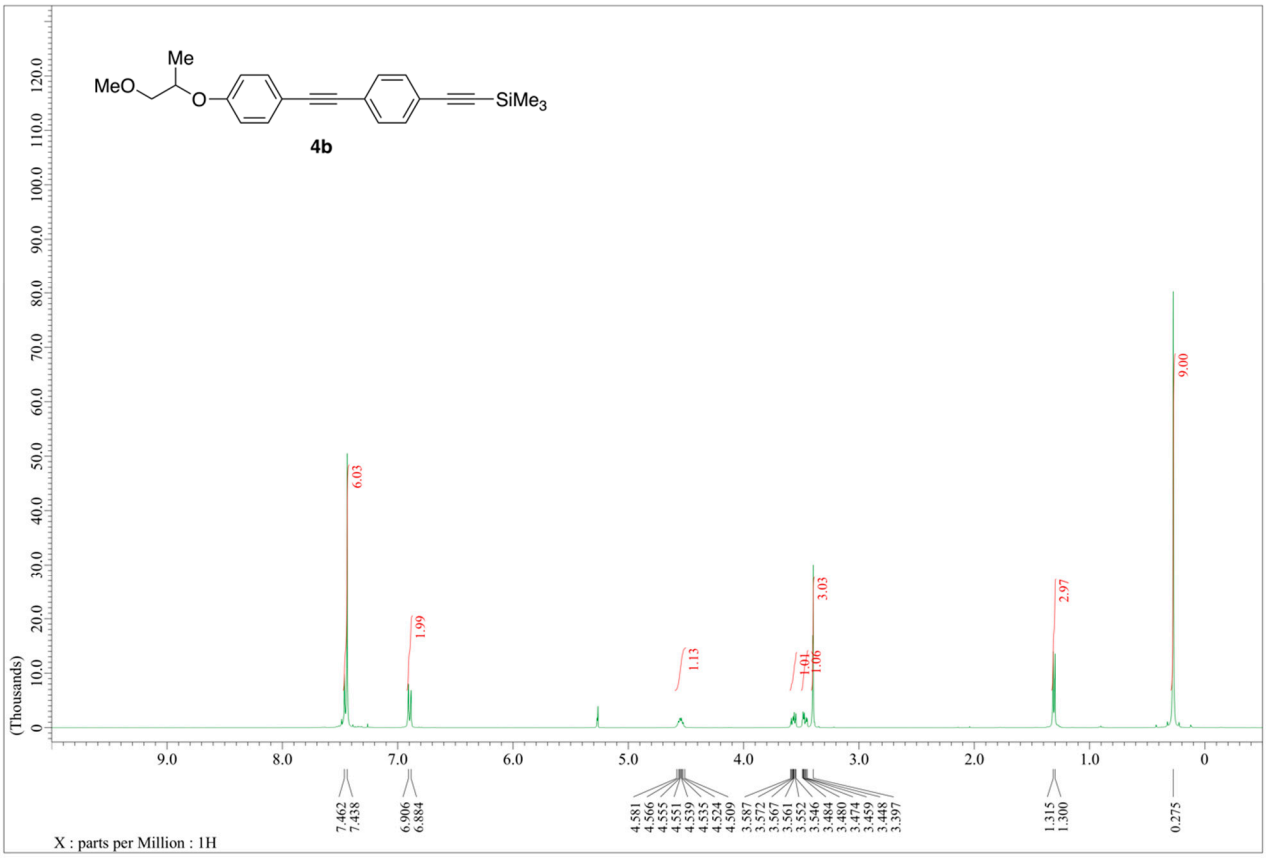

Figure S3. ^{1}H NMR spectrum of **4b** (Solvent: $CDCl_3$)

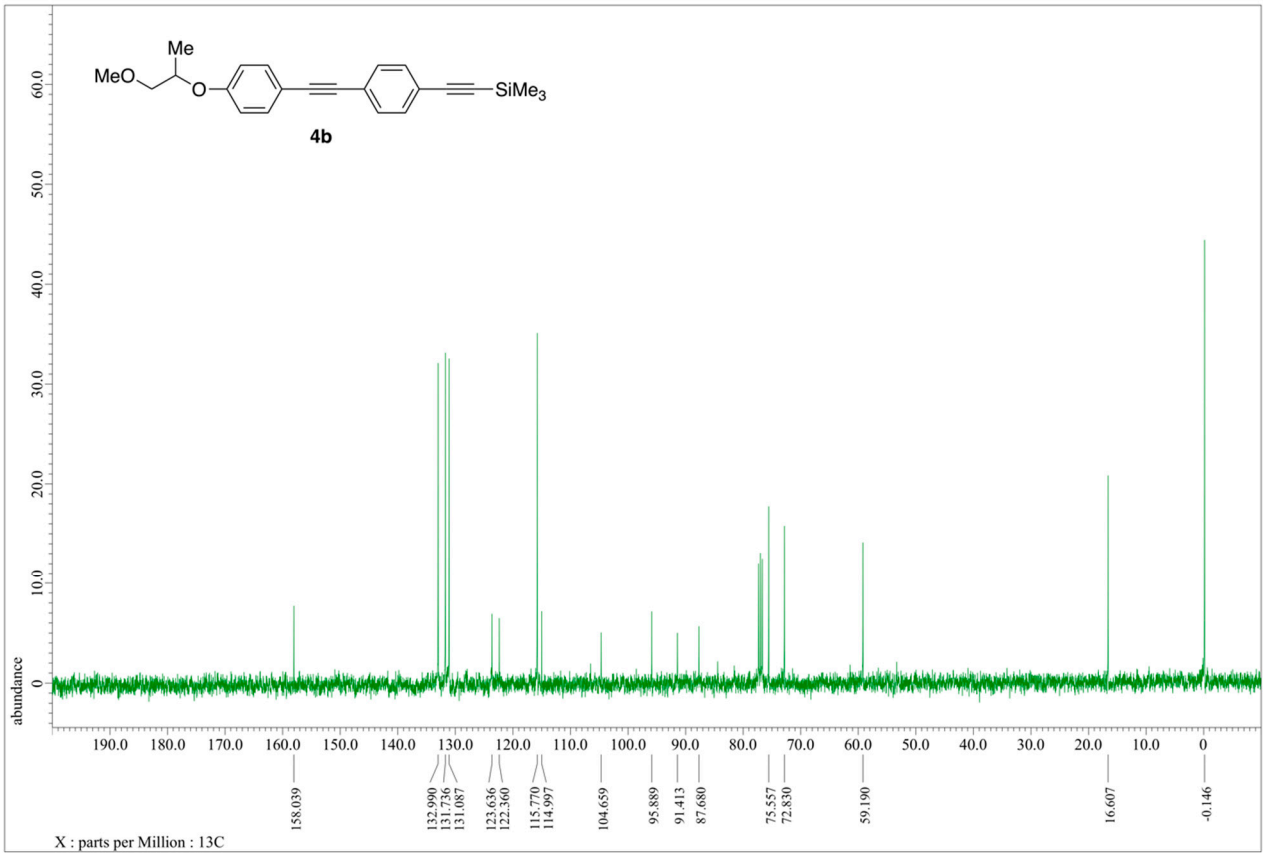

Figure S4. ^{13}C NMR spectrum of **4b** (Solvent: $CDCl_3$)

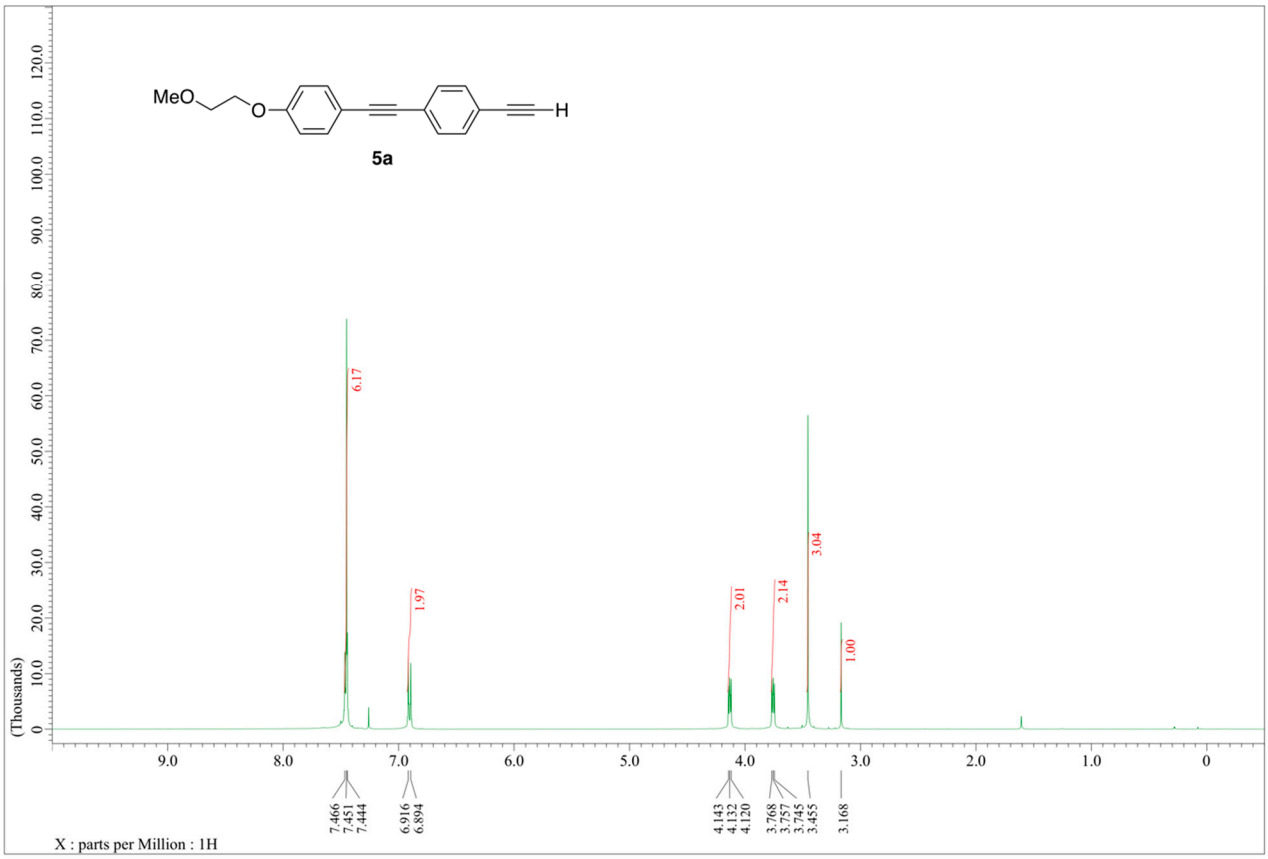

Figure S5. ^{1}H NMR spectrum of **5a** (Solvent: $CDCl_3$)

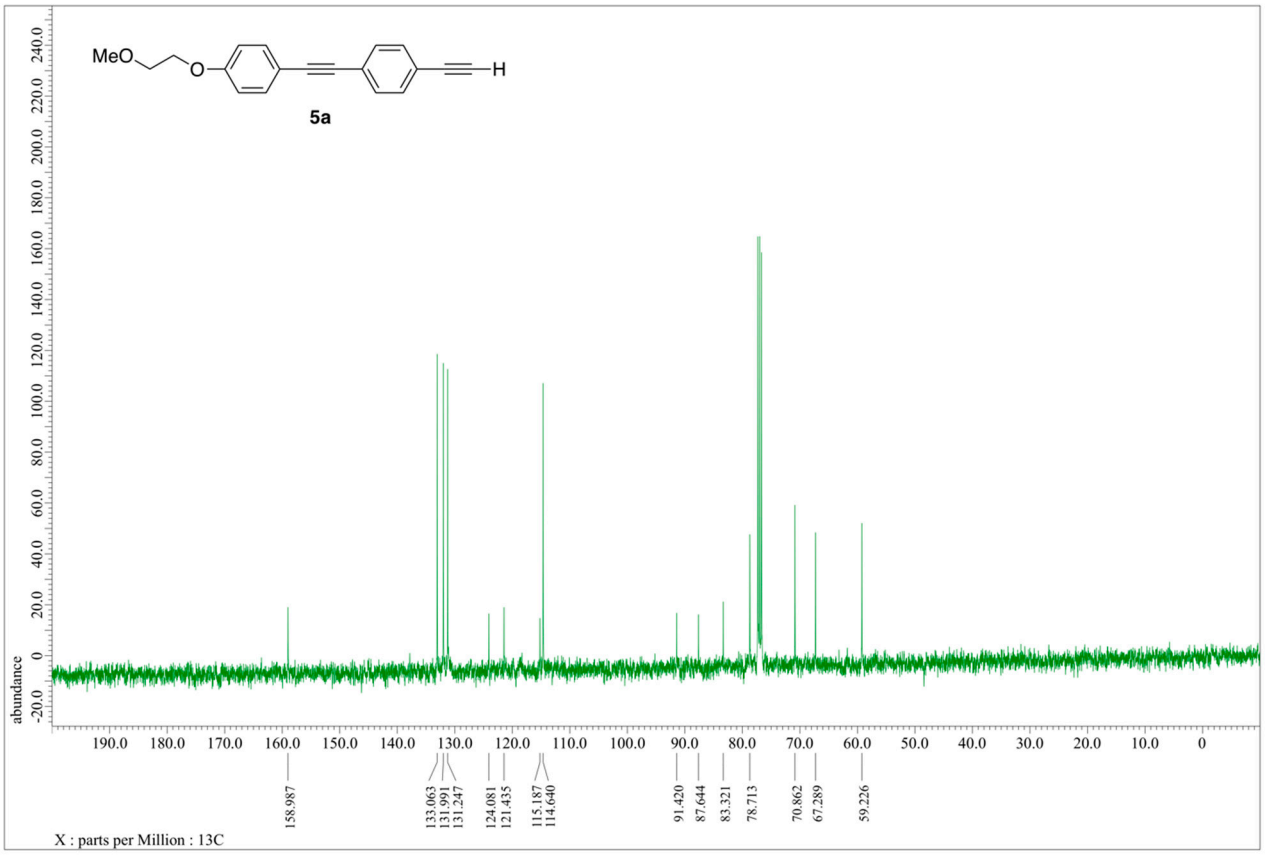

Figure S6. ^{13}C NMR spectrum of **5a** (Solvent: $CDCl_3$)

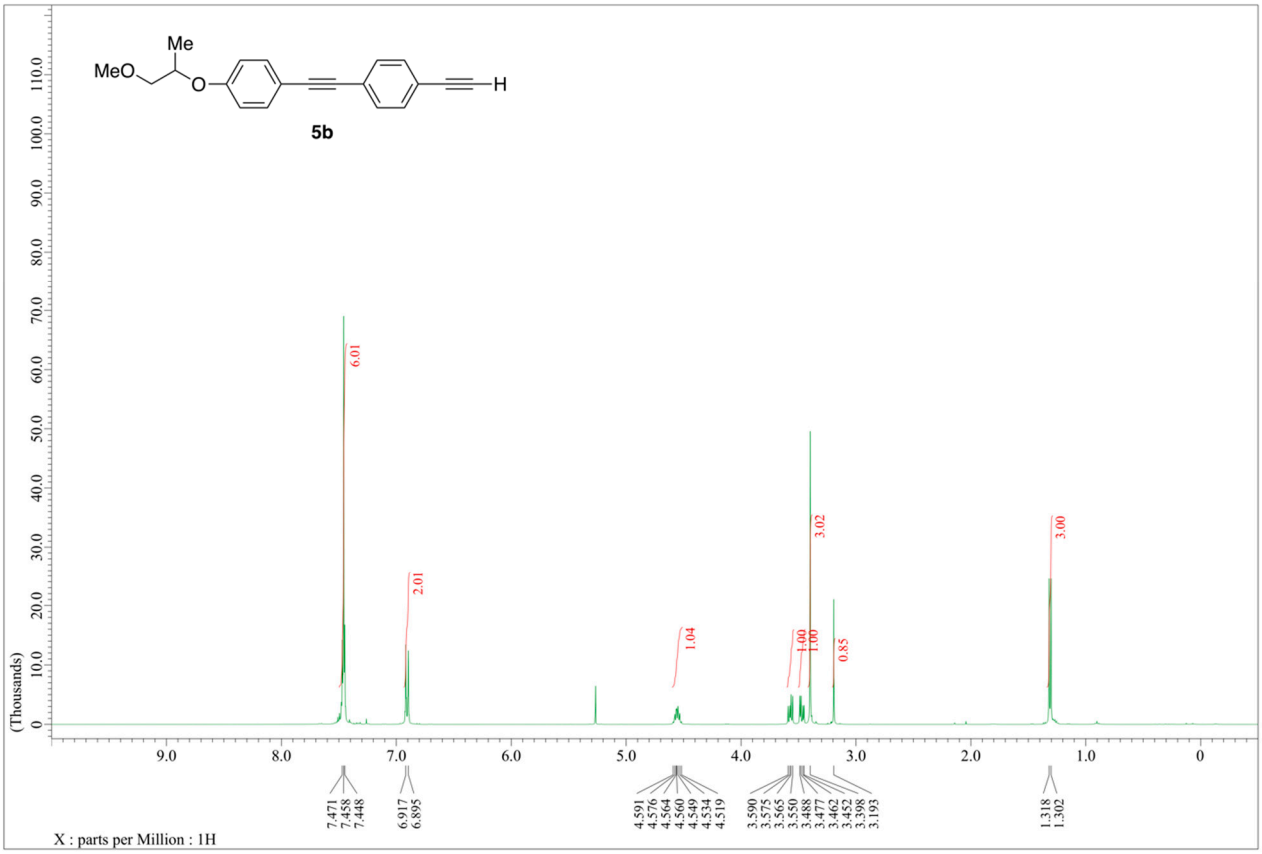

Figure S7. ^{1}H NMR spectrum of **5b** (Solvent: $CDCl_3$)

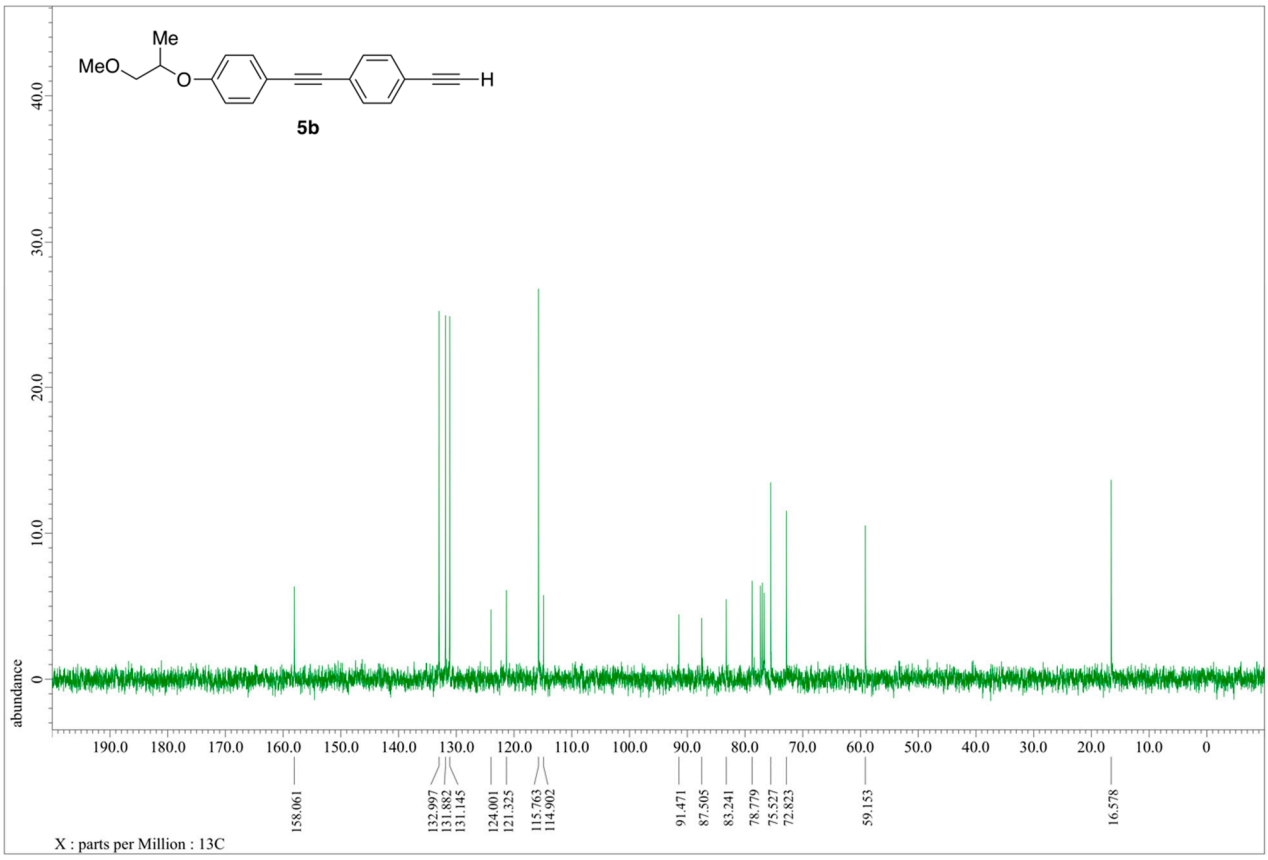

Figure S8. ^{13}C NMR spectrum of **5b** (Solvent: $CDCl_3$)

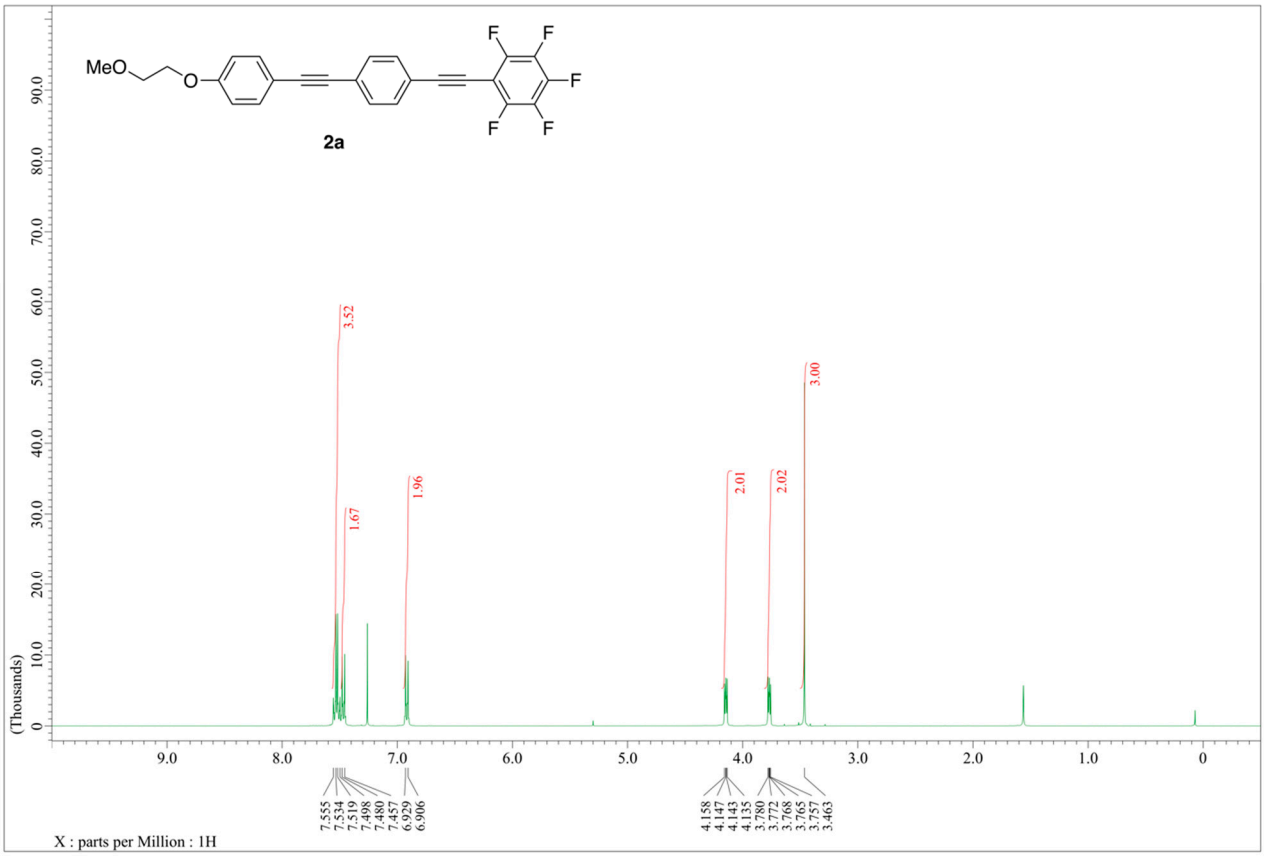

Figure S9. ^{1}H NMR spectrum of **2a** (Solvent: $CDCl_3$)

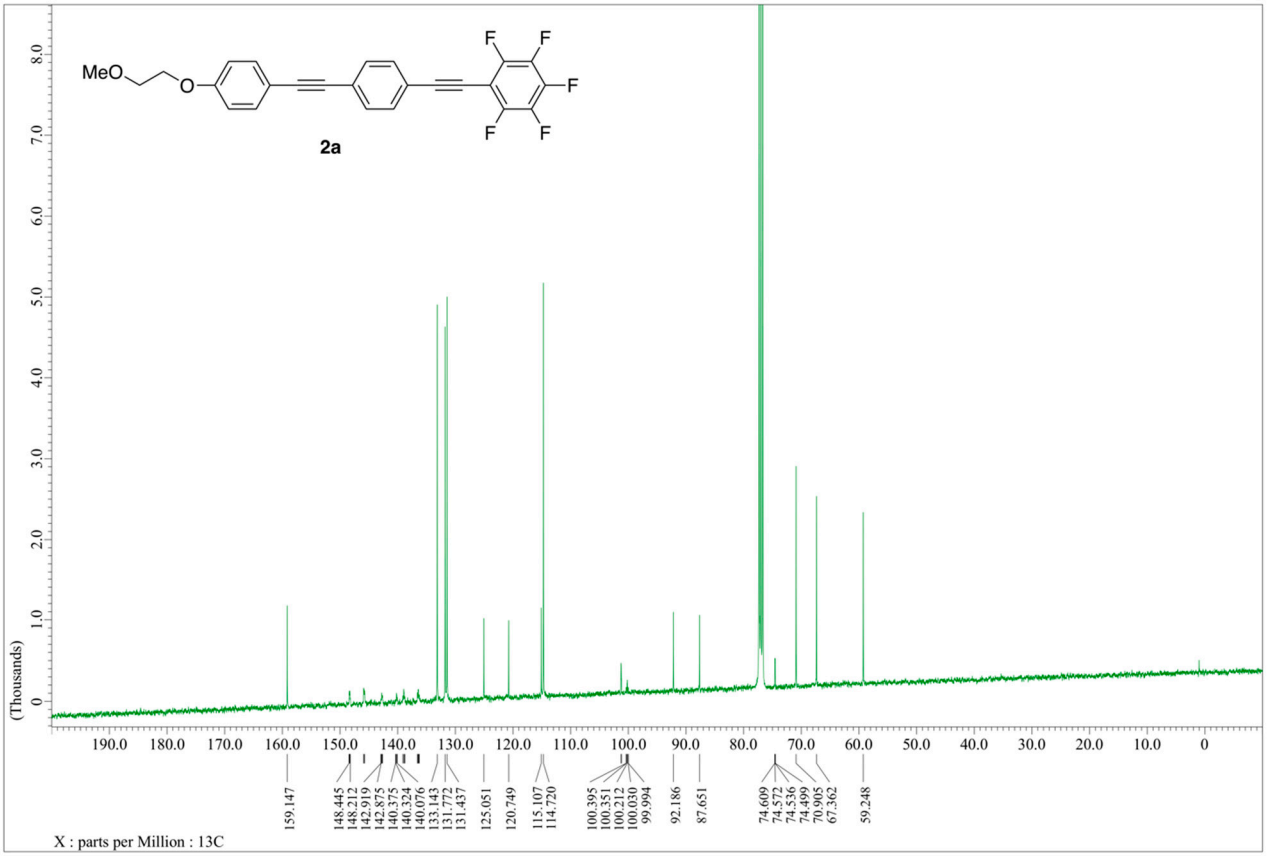

Figure S10. ^{13}C NMR spectrum of **2a** (Solvent: $CDCl_3$)

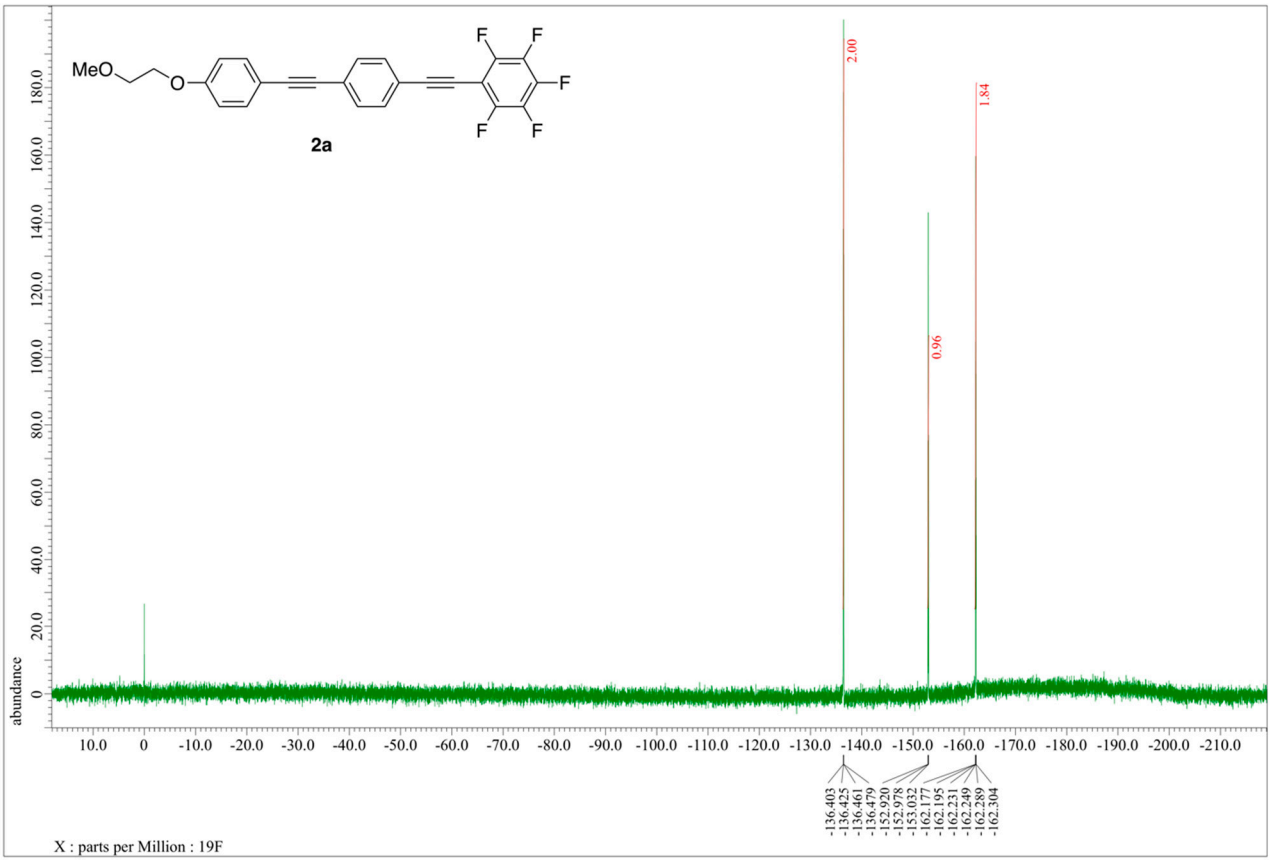

Figure S11. ^{19}F NMR spectrum of **2a** (Solvent: $CDCl_3$)

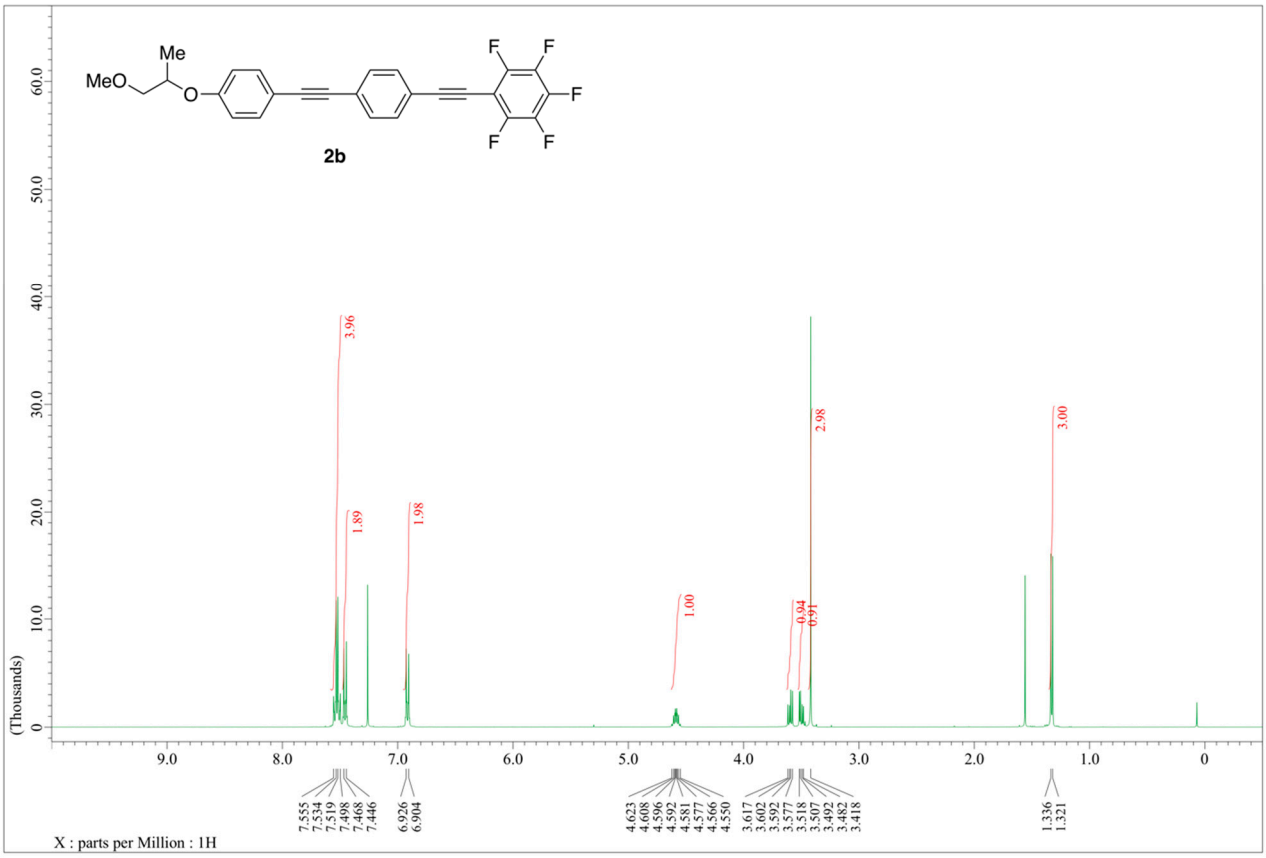

Figure S12. ^{1}H NMR spectrum of **2b** (Solvent: $CDCl_3$)

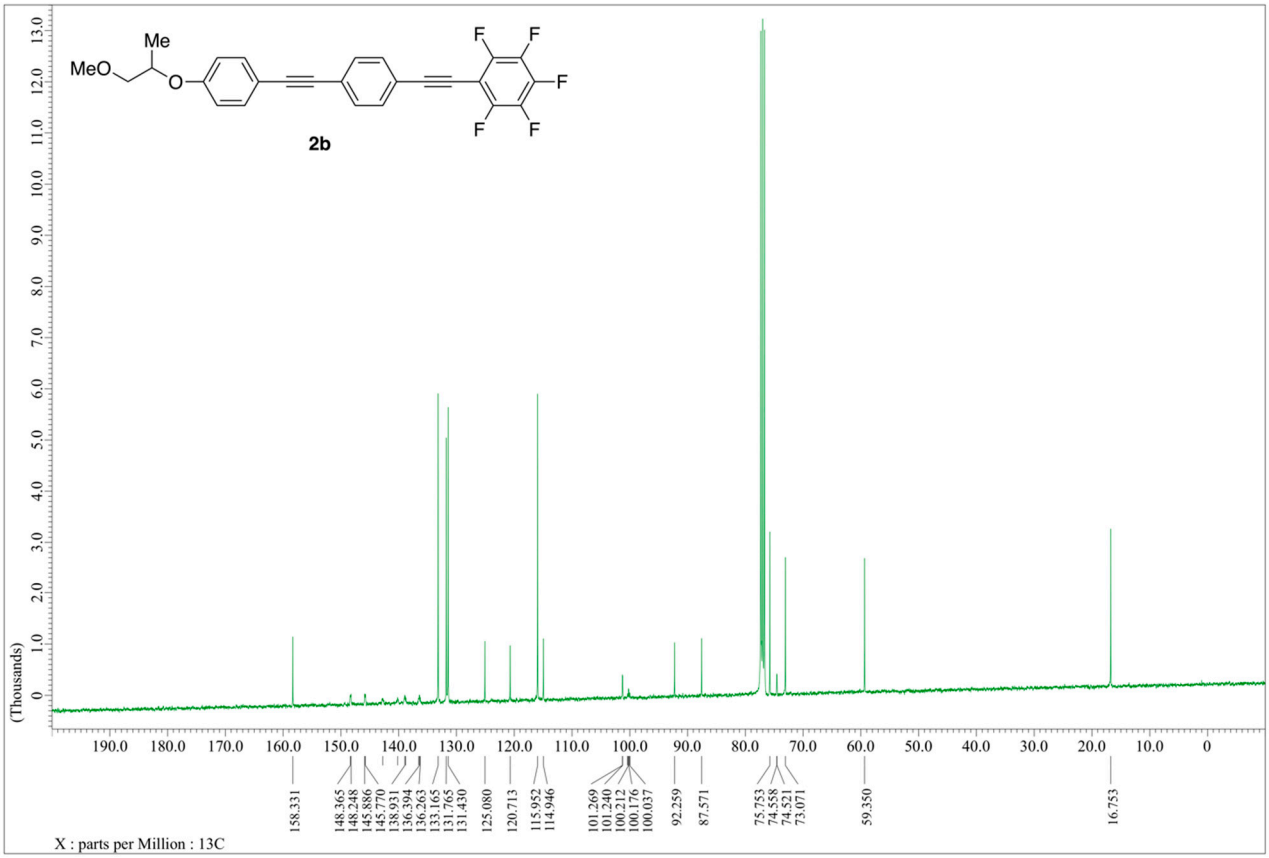

Figure S13. ^{13}C NMR spectrum of **2b** (Solvent: $CDCl_3$)

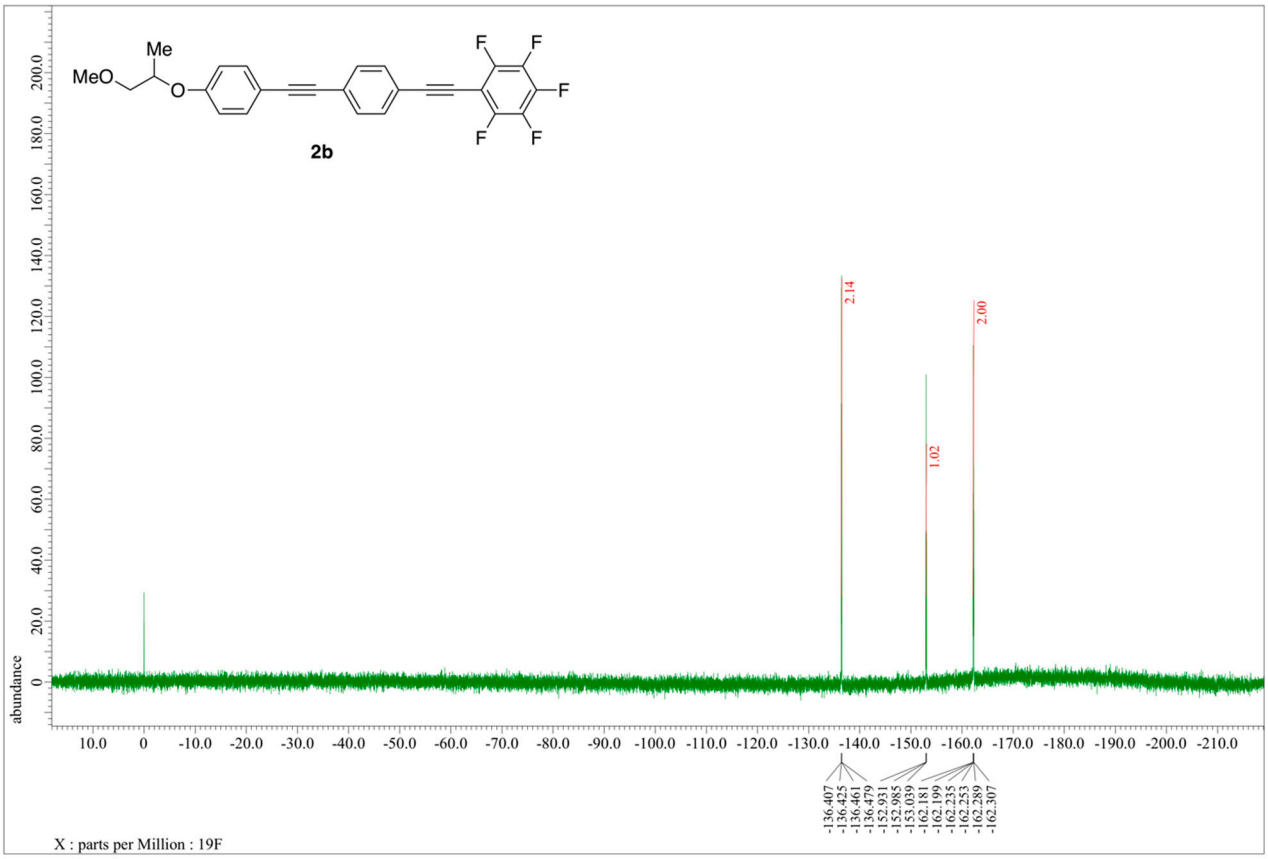

Figure S14. ^{19}F NMR spectrum of **2b** (Solvent: $CDCl_3$)

2. Quantum chemical calculation

All computations were performed using density functional theory (DFT) and the Gaussian 16 (Revision B.01) software package. Geometry optimizations were executed using the M06-2X hybrid functional [28,29] and the 6-31+G(d) basis set with the implicit solvation model (conductor-like polarizable continuum model (CPCM)) for CH_2Cl_2. The vertical excitation energies and dipole moments of optimized structures were calculated using the time-dependent DFT (TD-DFT) method at the same level of theory.

Optimized Geometry

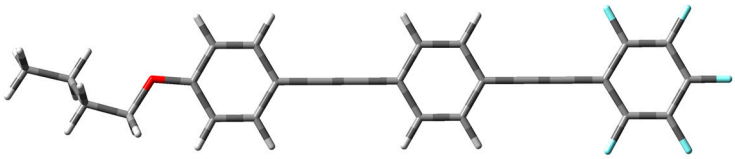

E(RM062X) = –1574.73458654 Hartree

Dipole moment (Debye): X= –5.2751 Y= –1.5649 Z= –0.0821 Tot= 5.5029

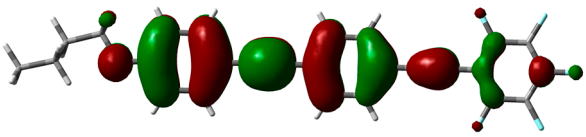

HOMO (–7.05 eV)

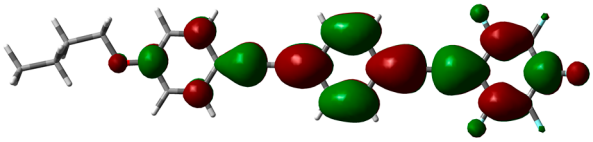

LUMO (–1.59 eV)

Figure S15. Optimized Geometry, HOMO and LUMO Distribution of **1**.

Table S1. Cartesian Coordinates of **1** (S_0 state)

No.	Atom No.	Type	Coordinates (Angstroms) x	y	z
1	9	0	6.29777	–2.36298	–0.060468
2	9	0	8.99325	–2.37133	–0.130045
3	9	0	10.36130	–0.024565	–0.147898
4	6	0	–11.55120	0.260594	–0.921350
5	1	0	–10.94830	1.17512	–0.955645
6	1	0	–11.33870	–0.292236	–1.84618
7	9	0	6.32519	2.35937	–0.024719
8	6	0	–11.11950	–0.585471	0.275632
9	1	0	–11.7170	–1.50540	0.313703
10	1	0	–11.31090	–0.041968	1.20999
11	8	0	–8.87340	0.201008	0.306371
12	6	0	–9.65825	–0.988738	0.232030
13	1	0	–9.40399	–1.64344	1.07500
14	9	0	9.02052	2.33751	–0.095046
15	6	0	–7.52497	0.087639	0.270798
16	6	0	–6.83792	–1.12699	0.163971
17	1	0	–7.36892	–2.06937	0.102195
18	6	0	–5.44529	–1.12796	0.136067
19	1	0	–4.91413	–2.07135	0.052745
20	6	0	–4.71839	0.066729	0.213468
21	6	0	–5.42374	1.28087	0.321329
22	1	0	–4.87363	2.21494	0.382692
23	6	0	–6.80688	1.29093	0.349790
24	1	0	–7.35836	2.22224	0.433128
25	6	0	–3.28784	0.055308	0.183076
26	6	0	–2.07377	0.048441	0.156674
27	6	0	–0.643533	0.039784	0.124544
28	6	0	0.058494	–1.17498	0.036658
29	1	0	–0.493197	–2.10861	–0.006506
30	6	0	1.44511	–1.18398	0.004863
31	1	0	1.98366	–2.12391	–0.063252
32	6	0	2.16120	0.023213	0.059850
33	6	0	1.46272	1.23876	0.147847
34	1	0	2.01490	2.17223	0.190687
35	6	0	0.076095	1.24612	0.180007
36	1	0	–0.461971	2.18620	0.248171
37	6	0	3.59102	0.014661	0.025697
38	6	0	4.80254	0.006894	–0.004656
39	6	0	6.22451	–0.001315	–0.040463
40	6	0	6.96051	1.18864	–0.050010
41	6	0	8.34530	1.18938	–0.086189
42	6	0	9.03295	–0.017069	–0.113330
43	6	0	8.33135	–1.21572	–0.104414
44	6	0	6.94663	–1.19945	–0.068409
45	1	0	–9.42869	–1.51590	–0.704222
46	6	0	–13.03460	0.619987	–0.863934
47	1	0	–13.33300	1.22418	–1.72611
48	1	0	–13.65600	–0.282651	–0.853556
49	1	0	–13.26210	1.19218	0.042503

Table S2. Cartesian Coordinates of **1** (S_1 state)

No.	Atom No.	Type	Coordinates (Angstroms) x	y	z
1	9	0	6.26814	2.36942	0.098353
2	9	0	8.96471	2.37321	0.166137
3	9	0	10.34100	0.025555	0.145361
4	6	0	–11.50560	–0.241422	0.928109
5	1	0	–10.88910	–1.14477	1.00023
6	1	0	–11.30450	0.351058	1.83052
7	9	0	6.29900	–2.36637	–0.014399
8	6	0	–11.08450	0.562902	–0.301049
9	1	0	–11.69380	1.47261	–0.376173
10	1	0	–11.26560	–0.018451	–1.21419
11	8	0	–8.82687	–0.195156	–0.297306
12	6	0	–9.63094	0.99094	–0.270816
13	1	0	–9.37879	1.61023	–1.13956
14	9	0	8.99530	–2.33825	0.054728
15	6	0	–7.49312	–0.083366	–0.265596
16	6	0	–6.80091	1.14354	–0.204787
17	1	0	–7.33673	2.08486	–0.179923
18	6	0	–5.42051	1.14738	–0.176455
19	1	0	–4.88351	2.08946	–0.129348
20	6	0	–4.67907	–0.067894	–0.207646
21	6	0	–5.40269	–1.29843	–0.269720
22	1	0	–4.85161	–2.23308	–0.294680
23	6	0	–6.77507	–1.30100	–0.298138
24	1	0	–7.33606	–2.22886	–0.345944
25	6	0	–3.29109	–0.057403	–0.178588
26	6	0	–2.05053	–0.049718	–0.152111
27	6	0	–0.672932	–0.041034	–0.121969
28	6	0	0.058804	1.19977	–0.064103
29	1	0	–0.497519	2.13176	–0.045271
30	6	0	1.42294	1.20671	–0.033356
31	1	0	1.96714	2.14502	0.010340
32	6	0	2.16784	–0.023714	–0.056916
33	6	0	1.43991	–1.26308	–0.114822
34	1	0	1.99697	–2.19463	–0.133347
35	6	0	0.075817	–1.27280	–0.146634
36	1	0	–0.467632	–2.21151	–0.190861
37	6	0	3.55210	–0.015228	–0.024303
38	6	0	4.78496	–0.007416	0.005461
39	6	0	6.17973	0.000929	0.039645
40	6	0	6.93619	–1.19365	0.029598
41	6	0	8.31566	–1.18959	0.064766
42	6	0	9.00882	0.017656	0.111323
43	6	0	8.30002	1.21660	0.122104
44	6	0	6.92058	1.20436	0.087135
45	1	0	–9.40589	1.55203	0.645455
46	6	0	–12.98310	–0.625915	0.880981
47	1	0	–13.27380	–1.20055	1.76554
48	1	0	–13.61820	0.265800	0.834182
49	1	0	–13.19880	–1.23665	–0.002822

Optimized Geometry

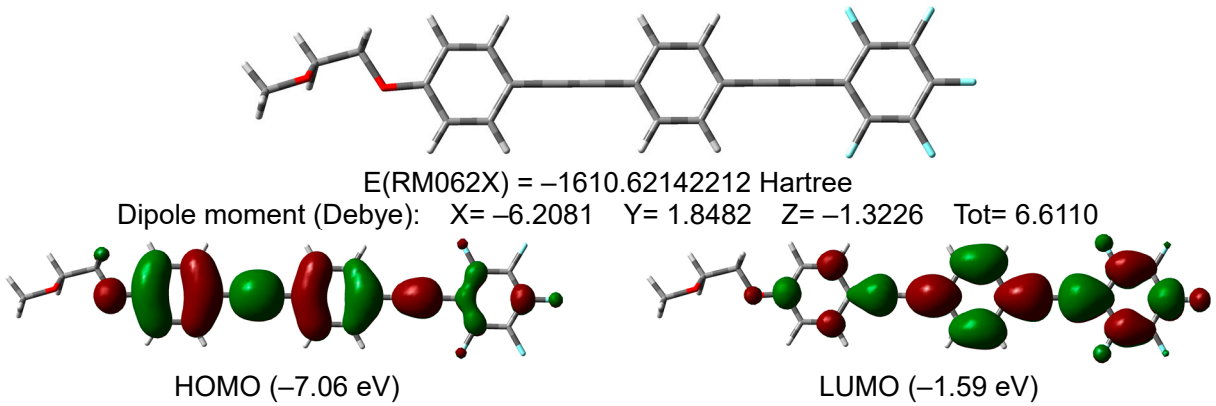

Figure S16. Optimized Geometry, HOMO and LUMO Distribution of **2a**.

Table S3. Cartesian Coordinates of **2a** (S_0 state)

No.	Atom No.	Type	Coordinates (Angstroms) x	y	z
1	9	0	6.27862	2.37089	0.054843
2	9	0	8.97437	2.38916	0.111756
3	9	0	10.35110	0.047481	0.126077
4	9	0	6.32317	–2.35136	0.024938
5	6	0	–11.11780	0.546570	–0.301847
6	1	0	–11.72900	1.45205	–0.435670
7	1	0	–11.29520	–0.119317	–1.15998
8	8	0	–8.88335	–0.244482	–0.299894
9	6	0	–9.66331	0.943441	–0.253004
10	1	0	–9.42509	1.58230	–1.11256
11	9	0	9.01871	–2.31958	0.082498
12	6	0	–7.53382	–0.127693	–0.258663
13	6	0	–6.85049	1.09032	–0.177354
14	1	0	–7.38272	2.03336	–0.139399
15	6	0	–5.45791	1.09454	–0.144509
16	1	0	–4.92877	2.04055	–0.081321
17	6	0	–4.72908	–0.10037	–0.191916
18	6	0	–5.43180	–1.31805	–0.273254
19	1	0	–4.87988	–2.25226	–0.310655
20	6	0	–6.81487	–1.33147	–0.305864
21	1	0	–7.36486	–2.26518	–0.368533
22	6	0	–3.29853	–0.085147	–0.159514
23	6	0	–2.08457	–0.073806	–0.133074
24	6	0	–0.654289	–0.059645	–0.102943
25	6	0	0.043283	1.15858	–0.028956
26	1	0	–0.511851	2.09050	0.006008
27	6	0	1.42993	1.17308	–0.000754
28	1	0	1.96511	2.11564	0.056397
29	6	0	2.15037	–0.031930	–0.045581
30	6	0	1.45629	–1.25094	–0.119149
31	1	0	2.01189	–2.18269	–0.153977
32	6	0	0.069615	–1.26381	–0.147612
33	1	0	–0.465092	–2.20653	–0.204928
34	6	0	3.58027	–0.017562	–0.016470
35	6	0	4.79186	–0.004698	0.008792
36	6	0	6.21393	0.008944	0.038240
37	6	0	6.95432	–1.17830	0.045851
38	6	0	8.33926	–1.17395	0.075453
39	6	0	9.02260	0.035052	0.097807
40	6	0	8.31657	1.23111	0.090680
41	6	0	6.93177	1.20976	0.061224
42	1	0	–9.45479	1.49236	0.673754
43	6	0	–12.80530	–0.526433	0.914148
44	1	0	–12.98550	–1.00786	1.87620
45	1	0	–13.48720	0.327538	0.801153
46	1	0	–12.99730	–1.24487	0.105856
47	8	0	–11.45830	–0.101821	0.901930

Table S4. Cartesian Coordinates of **2a** (S_1 state)

No.	Atom No.	Type	Coordinates (Angstroms) x	y	z
1	9	0	6.24984	2.37663	0.085888
2	9	0	8.94674	2.38845	0.143899
3	9	0	10.3295	0.044771	0.127914
4	9	0	6.29408	–2.35950	–0.007041
5	6	0	–11.08360	0.528328	–0.312648
6	1	0	–11.70850	1.42149	–0.463536
7	1	0	–11.25350	–0.158186	–1.15572
8	8	0	–8.83804	–0.232281	–0.296375
9	6	0	–9.63639	0.950688	–0.278442
10	1	0	–9.40403	1.56579	–1.15556
11	9	0	8.99062	–2.32331	0.052048
12	6	0	–7.50275	–0.11741	–0.258078
13	6	0	–6.81414	1.11094	–0.205972
14	1	0	–7.35094	2.05202	–0.191825
15	6	0	–5.43355	1.11763	–0.173044
16	1	0	–4.89858	2.06114	–0.133012
17	6	0	–4.69039	–0.096418	–0.190874
18	6	0	–5.41148	–1.32861	–0.243121
19	1	0	–4.85885	–2.26255	–0.257002
20	6	0	–6.78400	–1.33400	–0.275679
21	1	0	–7.34350	–2.26307	–0.315605
22	6	0	–3.30214	–0.082861	–0.159618
23	6	0	–2.06177	–0.071404	–0.132959
24	6	0	–0.684143	–0.058086	–0.104172
25	6	0	0.043355	1.18565	–0.056160
26	1	0	–0.516239	2.11575	–0.042519
27	6	0	1.40744	1.19750	–0.028342
28	1	0	1.94861	2.13786	0.007835
29	6	0	2.15645	–0.030693	–0.045551
30	6	0	1.43260	–1.27308	–0.092945
31	1	0	1.99288	–2.20277	–0.106205
32	6	0	0.068552	–1.28756	–0.121445
33	1	0	–0.471920	–2.22831	–0.157767
34	6	0	3.54051	–0.017292	–0.017191
35	6	0	4.77355	–0.005090	0.008338
36	6	0	6.16820	0.007642	0.037536
37	6	0	6.92808	–1.18491	0.029815
38	6	0	8.30761	–1.17669	0.059881
39	6	0	8.99735	0.032841	0.098808
40	6	0	8.28517	1.22986	0.107122
41	6	0	6.90570	1.21355	0.077195
42	1	0	–9.42956	1.52050	0.634974
43	6	0	–12.74260	–0.550378	0.937459
44	1	0	–12.90610	–1.01364	1.91121
45	1	0	–13.44200	0.286972	0.810357
46	1	0	–12.92420	–1.29044	0.146681
47	8	0	–11.40400	–0.098568	0.906857

Optimized Geometry

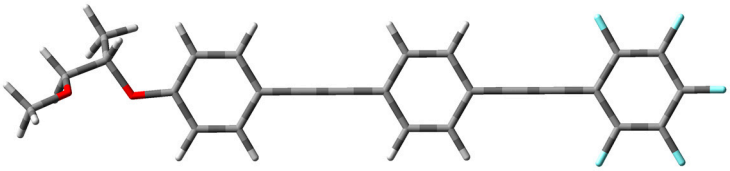

E(RM062X) = –1649.91910777 Hartree

Dipole moment (Debye): X= –6.7273 Y= 1.6553 Z= –0.8980 Tot= 6.9860

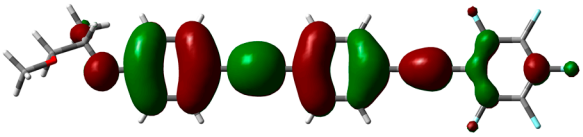

HOMO (–7.04 eV)

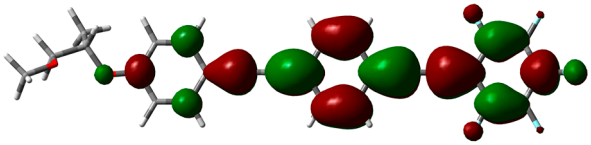

LUMO (–1.59 eV)

Figure S17. Optimized Geometry, HOMO and LUMO Distribution of *S*-**2b**.

Table S5. Cartesian Coordinates of *S*-**2b** (S_0 state)

No.	Atom No.	Type	Coordinates (Angstroms) x	y	z
1	9	0	6.54547	2.36492	0.289649
2	9	0	9.23927	2.40693	0.404034
3	9	0	10.64470	0.088762	0.232786
4	9	0	6.65025	–2.33410	–0.171114
5	6	0	–10.77850	0.247702	0.191804
6	1	0	–11.51090	1.06928	0.174836
7	1	0	–11.11060	–0.525721	–0.518887
8	8	0	-8.58380	–0.365598	–0.394865
9	6	0	–9.42758	0.780243	–0.240200
10	9	0	9.34367	–2.27846	–0.055886
11	6	0	–7.23652	–0.223281	–0.360615
12	6	0	–6.56174	0.988113	–0.166958
13	1	0	–7.09768	1.92171	–0.044135
14	6	0	–5.16980	1.00250	–0.134592
15	1	0	–4.65083	1.94423	0.016336
16	6	0	–4.42766	–0.174487	–0.296088
17	6	0	–5.11888	–1.38451	–0.494613
18	1	0	–4.55885	–2.30599	–0.621483
19	6	0	–6.50202	–1.40750	–0.526932
20	1	0	–7.04247	–2.33697	–0.676073
21	6	0	–2.99753	–0.147917	–0.260017
22	6	0	–1.78379	–0.127353	–0.226977
23	6	0	–0.353990	–0.103346	–0.185109
24	6	0	0.332328	1.11240	–0.020273
25	1	0	–0.231182	2.03521	0.073502
26	6	0	1.71842	1.13593	0.023623
27	1	0	2.24481	2.07647	0.151718
28	6	0	2.44975	–0.057376	–0.096369
29	6	0	1.76704	–1.27370	–0.262479
30	1	0	2.33100	–2.19640	–0.355530
31	6	0	0.380884	–1.29559	–0.306462
32	1	0	–0.145036	–2.23635	–0.434069
33	6	0	3.87894	–0.033676	–0.046736
34	6	0	5.08981	–0.011922	–0.001046
35	6	0	6.51092	0.013826	0.055714
36	6	0	7.26592	–1.16105	–0.030183
37	6	0	8.64990	–1.14443	0.027817
38	6	0	9.31736	0.064707	0.175289
39	6	0	8.59659	1.24877	0.262680
40	6	0	7.21303	1.21520	0.202906
41	1	0	–9.03546	1.40732	0.569926
42	6	0	–11.89330	–0.839531	1.93834
43	1	0	–11.72530	–1.22411	2.94522
44	1	0	–12.68260	–0.075867	1.96764
45	1	0	–12.21640	–1.66064	1.28430
46	8	0	–10.67290	–0.287943	1.48955
47	6	0	–9.52868	1.55360	–1.54786
48	1	0	–8.53983	1.83697	–1.91740
49	1	0	–10.01530	0.937321	–2.31074
50	1	0	–10.11570	2.46544	–1.40580

Table S6. Cartesian Coordinates of *S*-**2b** (S_1 state)

No.	Atom No.	Type	Coordinates (Angstroms) x	y	z
1	9	0	6.51222	2.37405	0.302138
2	9	0	9.20706	2.41318	0.413961
3	9	0	10.62170	0.095648	0.230466
4	9	0	6.62226	–2.33713	–0.182959
5	6	0	–10.73920	0.248870	0.189915
6	1	0	–11.47880	1.06330	0.156430
7	1	0	–11.07010	–0.547053	–0.495769
8	8	0	–8.53993	–0.362437	–0.384476
9	6	0	–9.39891	0.784232	–0.268830
10	9	0	9.31646	–2.27365	–0.068968
11	6	0	–7.20748	–0.224905	–0.354055
12	6	0	–6.52572	1.00078	–0.201030
13	1	0	–7.06471	1.93611	–0.109804
14	6	0	–5.14599	1.01588	–0.170313
15	1	0	–4.61965	1.95782	–0.052858
16	6	0	–4.39082	–0.185189	–0.292277
17	6	0	–5.10195	–1.41383	–0.450667
18	1	0	–4.54220	–2.33879	–0.545666
19	6	0	–6.47433	–1.42736	–0.481089
20	1	0	–7.02569	–2.35478	–0.598269
21	6	0	–3.00331	–0.161108	–0.258190
22	6	0	–1.76307	–0.139066	–0.225023
23	6	0	–0.385927	–0.113318	–0.185424
24	6	0	0.326791	1.12994	–0.028633
25	1	0	–0.243458	2.04988	0.055216
26	6	0	1.69041	1.15399	0.014615
27	1	0	2.22018	2.09410	0.133254
28	6	0	2.45363	–0.060346	–0.094223
29	6	0	1.74482	–1.30186	–0.252788
30	1	0	2.31578	–2.22136	–0.336495
31	6	0	0.381245	–1.32870	–0.297165
32	1	0	–0.147734	–2.26916	–0.416436
33	6	0	3.83733	–0.034476	–0.045532
34	6	0	5.06940	–0.010366	0.000636
35	6	0	6.46340	0.016441	0.055697
36	6	0	7.23934	–1.16193	–0.036485
37	6	0	8.61793	–1.13977	0.020750
38	6	0	9.29051	0.070319	0.173824
39	6	0	8.56207	1.25380	0.267437
40	6	0	7.18370	1.22342	0.209344
41	1	0	–9.00602	1.44190	0.515071
42	6	0	–11.82210	–0.794832	1.98241
43	1	0	–11.63610	–1.14966	2.99686
44	1	0	–12.61540	–0.035347	2.00188
45	1	0	–12.14860	–1.63589	1.35624
46	8	0	–10.61170	–0.247877	1.50014
47	6	0	–9.50675	1.50006	–1.60720
48	1	0	–8.52182	1.78967	–1.98241
49	1	0	–9.97717	0.844541	–2.34667
50	1	0	–10.11270	2.40415	–1.50183

3. Phase transition behavior

Phase transition behavior of the present bistolanes were observed via polarizing optical microscopy (POM) using an Olympus BX53 microscope (Tokyo, Japan) equipped with a cooling and heating stage (Linkam Scientific Instruments, 10002L; Surrey, UK). The thermodynamic behavior was determined using a differential scanning calorimeter (DSC, SHIMADZU DSC-60 Plus; Kyoto, Japan) at heating and cooling rates of 5.0 °C min^{-1} under nitrogen atmosphere.

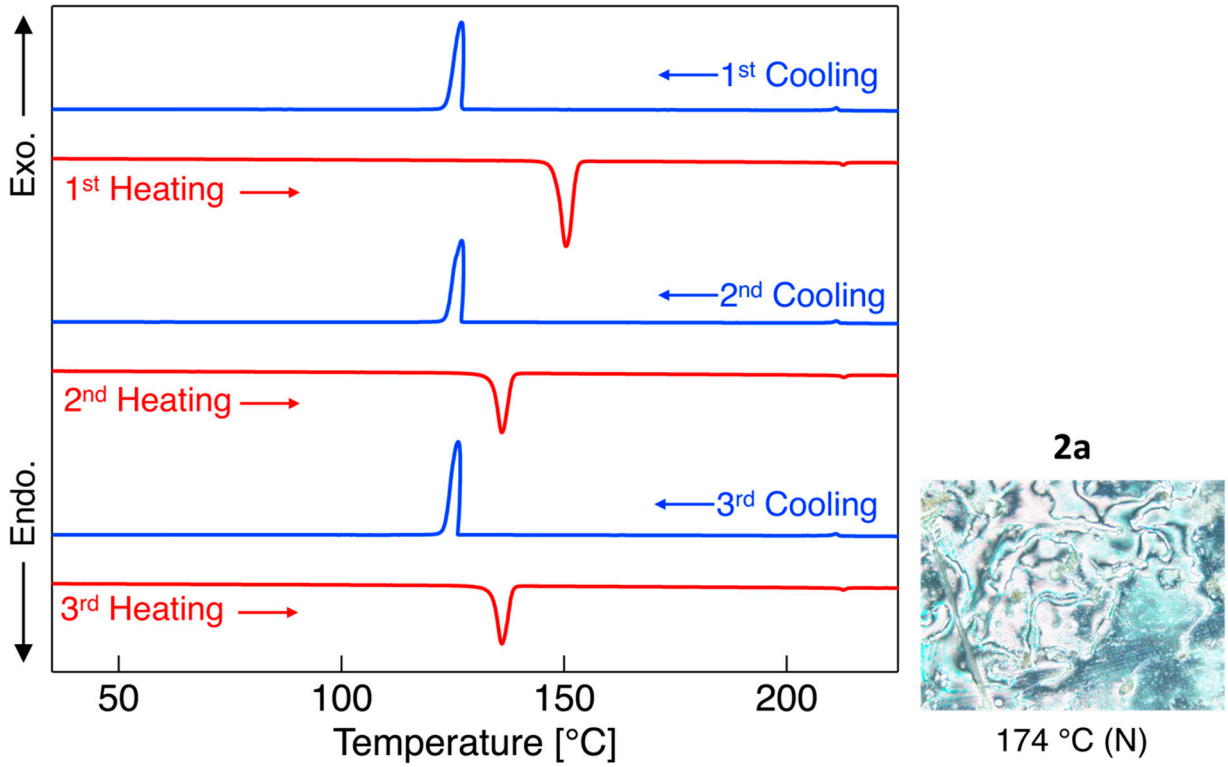

Figure 18. DSC thermogram of **2a** under N_2 atmosphere (scan rate: 5.0 °C min^{-1}) and POM image in nematic (N) phase observed at 174 °C on the 2nd cooling step.

Table S7. Phase transition behavior of **2a** determined by DSC

	Phase transition	Temperature [°C]	Enthalpy (ΔH) [kJ mol^{-1}]	Entropy (ΔS) [J mol^{-1} K^{-1}]
1st Heating	Cr–N N–Iso	148 212	41.1 0.48	97.7 0.99
1st Cooling	Cr–N N–Iso	127 212	–26.7 –0.50	–66.8 –1.04
2nd Heating	Cr–N N–Iso	134 212	27.3 0.58	67.2 1.19
2nd Cooling	Cr–N N–Iso	127 212	–26.2 –0.49	–65.5 –1.01
3rd Heating	Cr–N N–Iso	134 212	26.9 0.56	66.0 1.16
3rd Cooling	Cr–N N–Iso	127 212	–25.8 –0.49	–64.8 –1.01

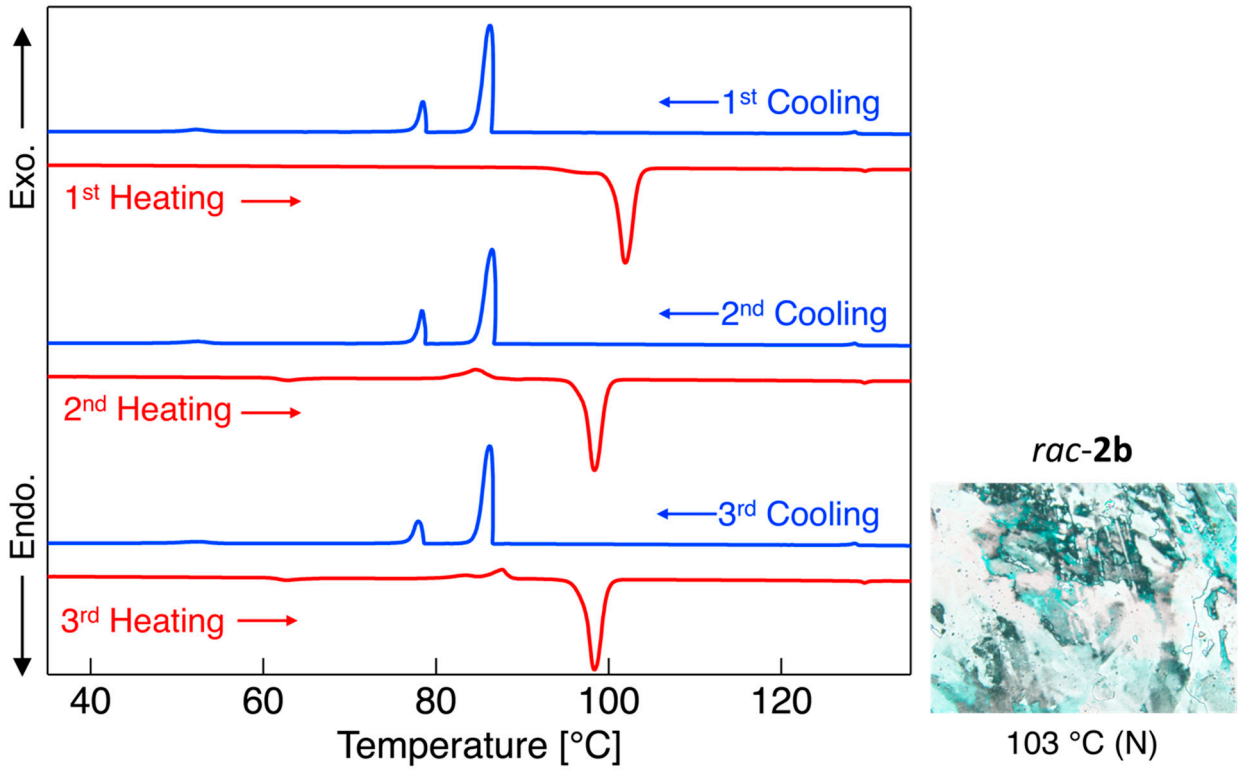

Figure S19. DSC thermogram of *rac*-**2b** under N_2 atmosphere (scan rate: 5.0 °C min^{-1}) and POM image in nematic (N) phase observed at 103 °C on the 2nd cooling step.

Table S8. Phase transition behavior of *rac*-**2b** determined by DSC

	Phase transition	Temperature [°C]	Enthalpy (ΔH) [kJ mol^{-1}]	Entropy (ΔS) [J mol^{-1} K^{-1}]
1st Heating	Cr–N	100	34.5	92.4
	N–Iso	129	0.30	0.75
1st Cooling	Cr^1–Cr^2	54	–0.97	–2.97
	Cr^2–Cr^3	79	–4.30	–12.2
	Cr^3–N	86	–17.4	–48.4
	N–Iso	129	–0.30	–0.75
2nd Heating	Cr^1–Cr^2	61	1.21	3.63
	Cr^2–Cr^3	82	–5.64	–15.9
	Cr^3–N	97	28.9	78.0
	N–Iso	129	0.23	0.57
2nd Cooling	Cr^1–Cr^2	54	–0.79	–2.42
	Cr^2–Cr^3	79	–4.40	–12.5
	Cr^3–N	87	–17.5	–48.5
	N–Iso	129	–0.29	–0.72
3rd Heating	Cr^1–Cr^2	61	1.07	3.21
	Cr^2–Cr^3	82	–5.14	–14.3
	Cr^3–N	97	28.8	77.8
	N–Iso	129	0.25	0.62
3rd Cooling	Cr^1–Cr^2	54	–0.95	–2.90
	Cr^2–Cr^3	79	–4.35	–12.4
	Cr^3–N	87	–17.4	–48.5
	N–Iso	129	–0.30	–0.74

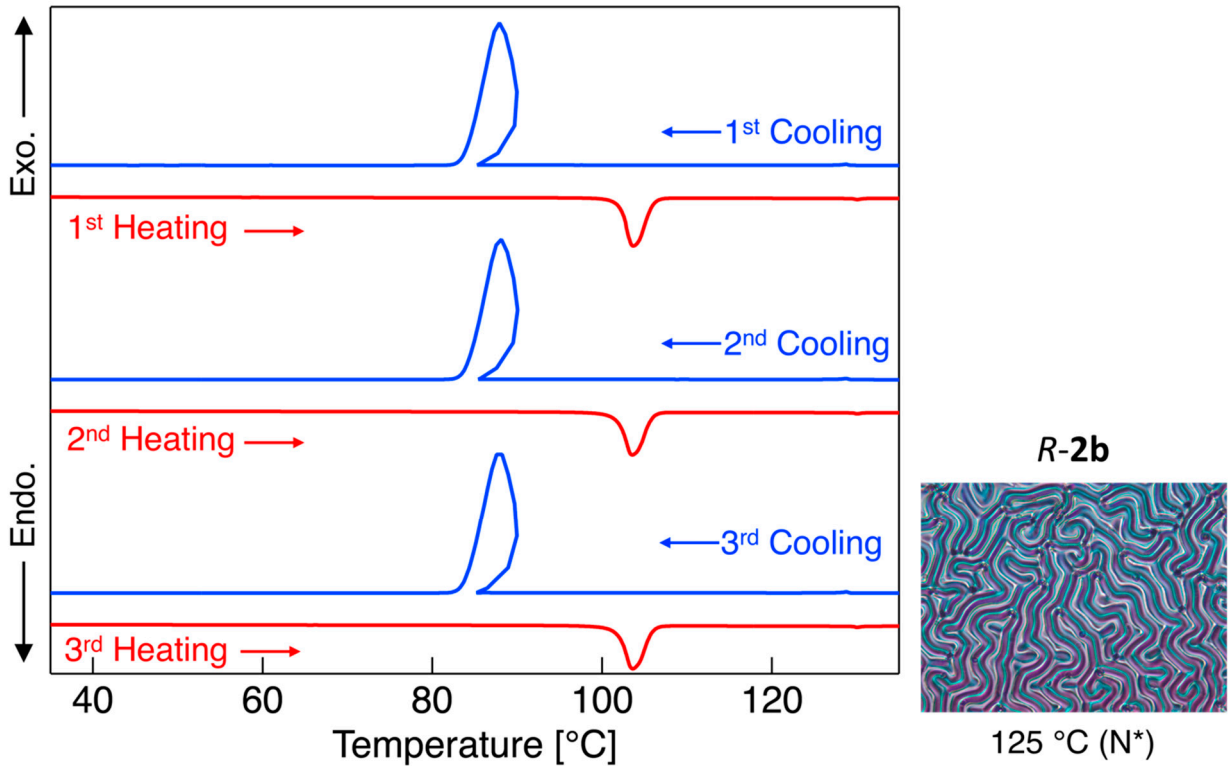

Figure S20. DSC thermogram of *R*-**2b** under N_2 atmosphere (scan rate: 5.0 °C min^{-1}) and POM image in chiral nematic (N*) phase observed at 125 °C on the 2nd cooling step.

Table S9. Phase transition behavior of *R*-**2b** determined by DSC

	Phase transition	Temperature [°C]	Enthalpy (ΔH) [kJ mol^{-1}]	Entropy (ΔS) [J mol^{-1} K^{-1}]
1st Heating	Cr–N* N*–Iso	102 130	119.6 1.01	319.1 2.53
1st Cooling	Cr–N* N*–Iso	85 130	–112.0 –1.00	–312.7 –2.50
2nd Heating	Cr–N* N*–Iso	102 130	117.1 0.88	312.5 2.18
2nd Cooling	Cr–N* N*–Iso	85 130	–111.9 –0.81	–312.2 –2.02
3rd Heating	Cr–N* N*–Iso	102 130	117.5 0.96	313.6 2.40
3rd Cooling	Cr–N* N*–Iso	85 130	–112.2 –0.99	–313.2 –2.47

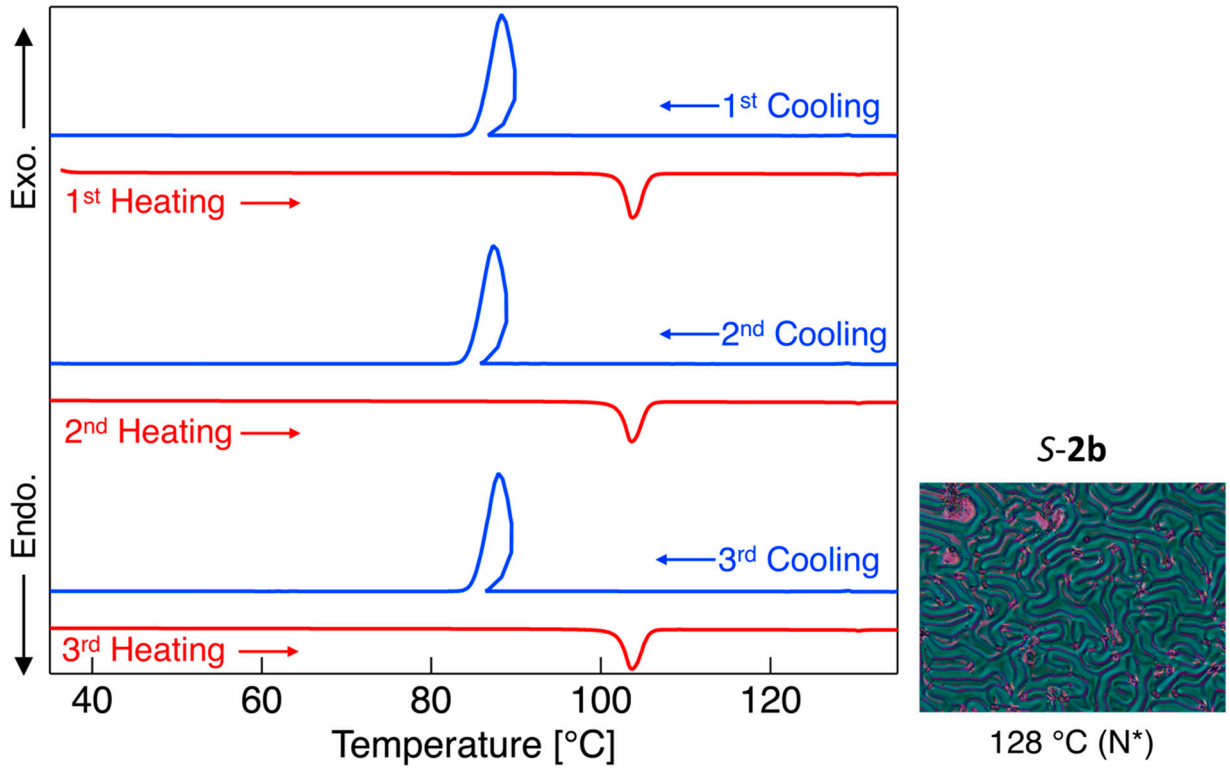

Figure S21. DSC thermogram of *S*-**2b** under N_2 atmosphere (scan rate: 5.0 °C min^{-1}) and POM image in chiral nematic (N*) phase observed at 128 °C on the 2nd cooling step.

Table S10. Phase transition behavior of *S*-**2b** determined by DSC

	Phase transition	Temperature [°C]	Enthalpy (ΔH) [kJ mol^{-1}]	Entropy (ΔS) [J mol^{-1} K^{-1}]
1st Heating	Cr–N* N*–Iso	102 130	33.6 0.27	89.6 0.68
1st Cooling	Cr–N* N*–Iso	85 130	–31.8 –0.25	–88.6 –0.62
2nd Heating	Cr–N* N*–Iso	102 130	32.9 0.35	87.6 0.86
2nd Cooling	Cr–N* N*–Iso	85 130	–31.7 –0.26	–88.4 –0.65
3rd Heating	Cr–N* N*–Iso	102 129	32.9 0.23	87.9 0.58
3rd Cooling	Cr–N* N*–Iso	85 130	–31.6 –0.26	–88.1 –0.66

4. PL behavior in CH_2Cl_2 solution

UV-vis absorption spectra were recorded on a JASCO V-500 absorption spectrometer (Tokyo, Japan). Samples for absorption measurements were prepared by dissolving crystalline **2a** or **2b** in a common organic solvent to a concentration of 1.0×10^{-5} mol L^{-1} and transferring the solution to a quartz cuvette with an optical path length of 1 cm. Steady-state photoluminescence (PL) spectra and PL quantum yields (PLQYs) in solution and crystalline states were obtained using a JASCO FP-6000 fluorescence spectrometer (Tokyo, Japan) and an absolute PLQY measurement system (Hamamatsu Photonics KK., C11347-01, Hamamatsu, Japan). PL measurements were performed for 1.0×10^{-6} mol L^{-1} solutions using quartz cuvettes with an optical path length of 1 cm. The excitation wavelength (λ_{ex}) corresponded to the maximum absorption wavelength.

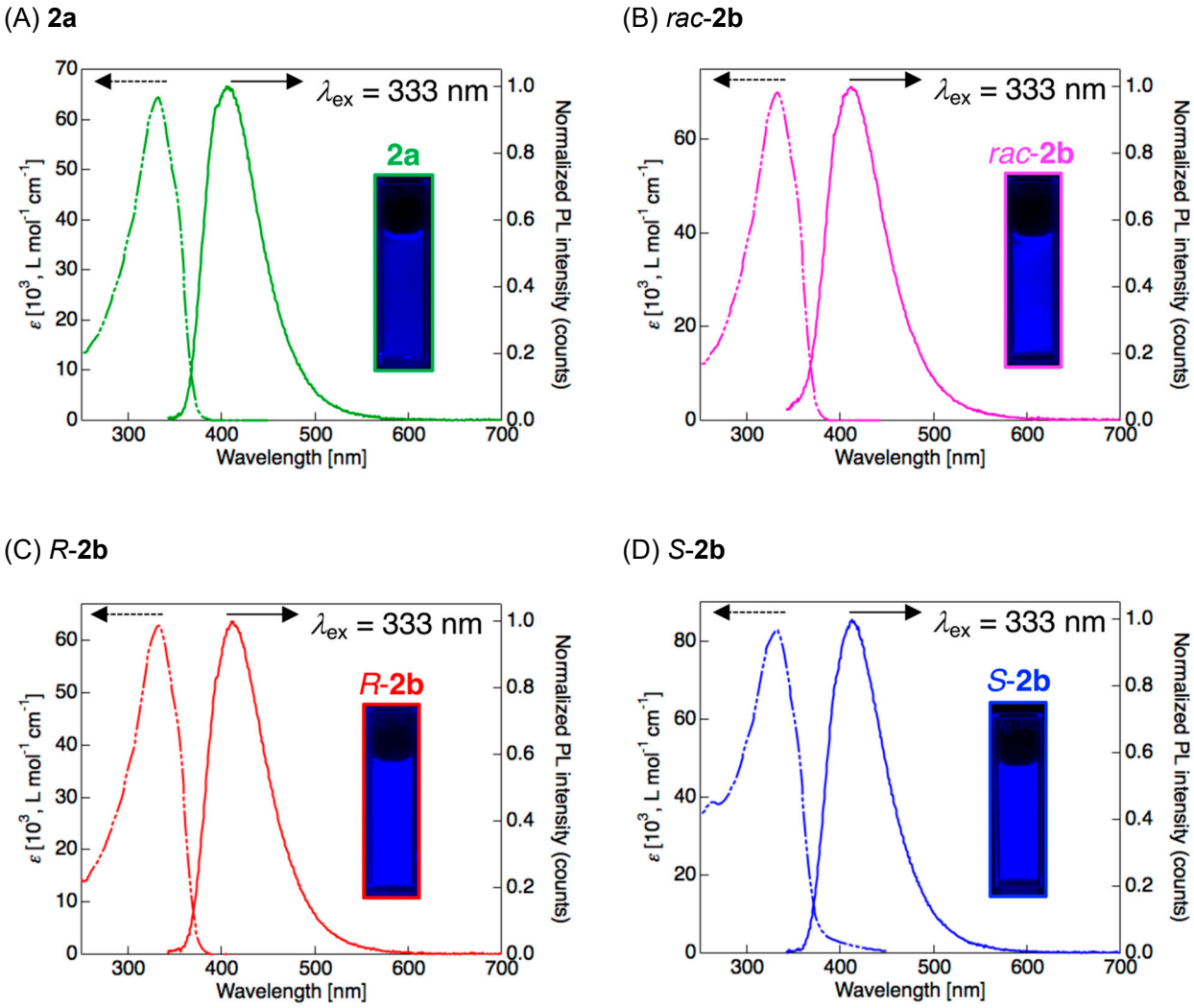

Figure S22. Absorption and PL spectra of (A) **2a**, (B) *rac*-**2b**, (C) *R*-**2b**, and (D) *S*-**2b** in CH2Cl2 solution phase. Inset: Photographs of these solutions under UV irradiation (λ_{ex} = 365 nm).

5. PL behavior of *S*-2b in various solvents

(A) Toluene (ε = 2.38)

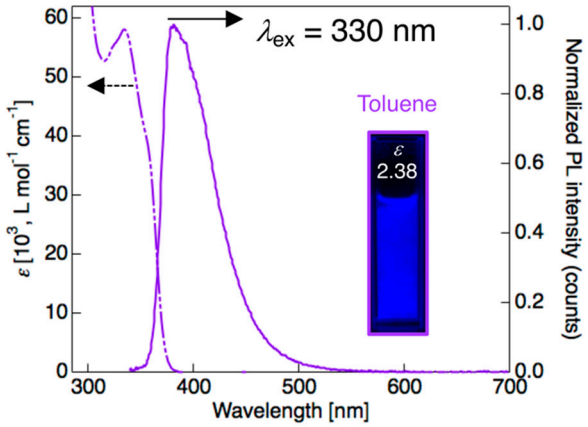

(B) $CHCl_3$ (ε = 4.81)

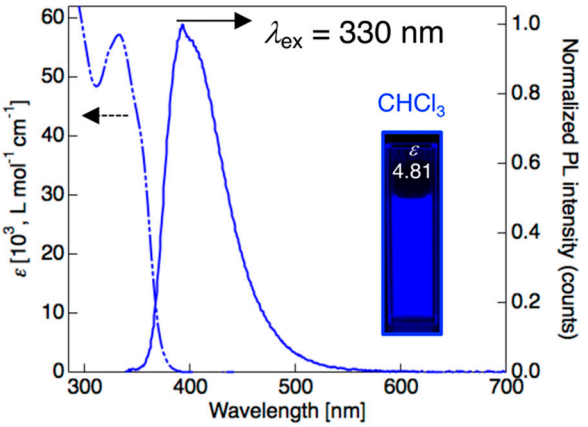

(C) THF (ε = 7.58)

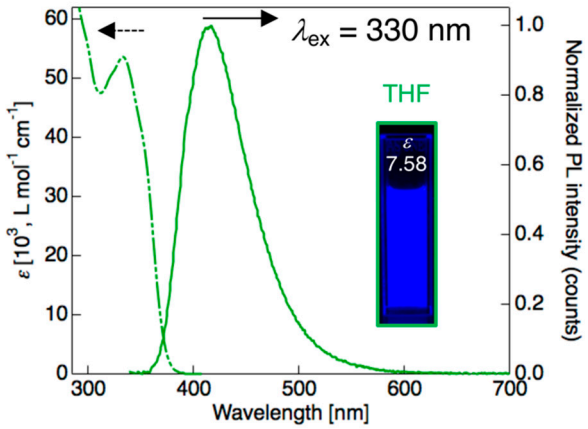

(D) MeCN (ε = 35.9)

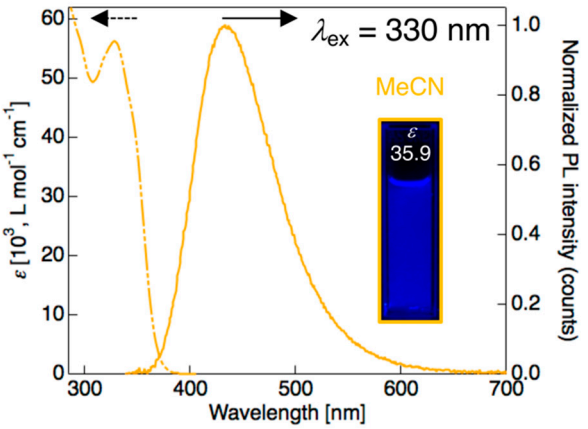

(E) DMF (ε = 36.7)

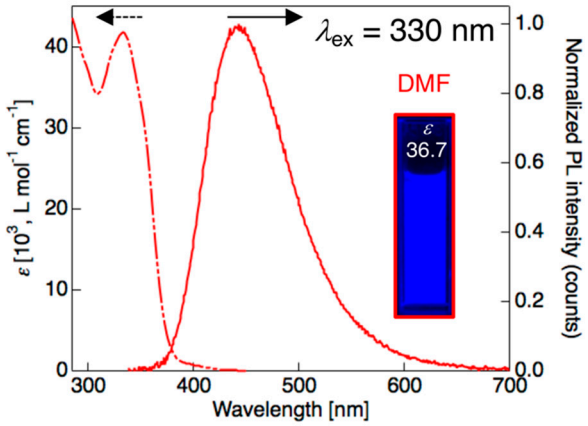

Figure S23. Absorption and PL spectra of *S*-**2b** in various solvent (ε: dielectric constant at 25 °C).

6. Lippert-Mataga plot

The Lippert-Mataga plot was constructed by using the relation

$$\nu_{abs} - \nu_{PL} = [2(\mu_e - \mu_g)^2/hca^3]\Delta f + (\nu_{abs} - \nu_{PL})^\circ \qquad (1)$$

where $\nu_{abs}-\nu_{PL}$ is the Stokes' shift, the superscript "°" indicates the absence of solvent, μ_g and μ_e are dipole moments in the ground and the excited states, respectively, D (1D = 1.0×10^{-18} $cm^{5/2}$ $g^{1/2}$ s^{-1}); h is the Planck constant ($h = 6.626\times10^{-27}$ erg s); c is the rate of light in vacuum ($c = 2.998\times10^{-10}$ cm s^{-1}). a is Onsager cavity radius. The Onsagar radius (a) was estimated by DFT calculation using Gaussian 16 with M06-2X/6-31+G(d) level of theory: a = 5.96 Å for *S*-**2b**. The orientation polarizability Δf is defined as

$$\Delta f = [(\varepsilon-1)/(2\varepsilon+1)] - [(n^2-1)/(2n^2+1)] \qquad (2)$$

where ε and n are solvent dielectric constant and refractive index, respectively.

Calculated values for Δf and Stokes shifts ($\nu_{abs}-\nu_{PL}$) for *S*-**2b** are summarized in Table S11.

Table S11. Polarizability and Stokes' shift obtained from general solvent effect.

				S-**2b**		
	ε	n	Δf	ν_{abs} [cm^{-1}]	ν_{PL} [cm^{-1}]	$\nu_{abs}-\nu_{PL}$
Toluene	2.38	1.496	0.013	29851	26247	3604
CH_2Cl_2	8.93	1.424	0.217	30030	24272	5758
$CHCl_3$	4.81	1.443	0.149	30030	25445	4585
THF	7.58	1.408	0.209	30030	23981	6049
DMF	36.71	1.428	0.275	29940	22831	7109
MeCN	35.94	1.344	0.305	30864	23256	7608

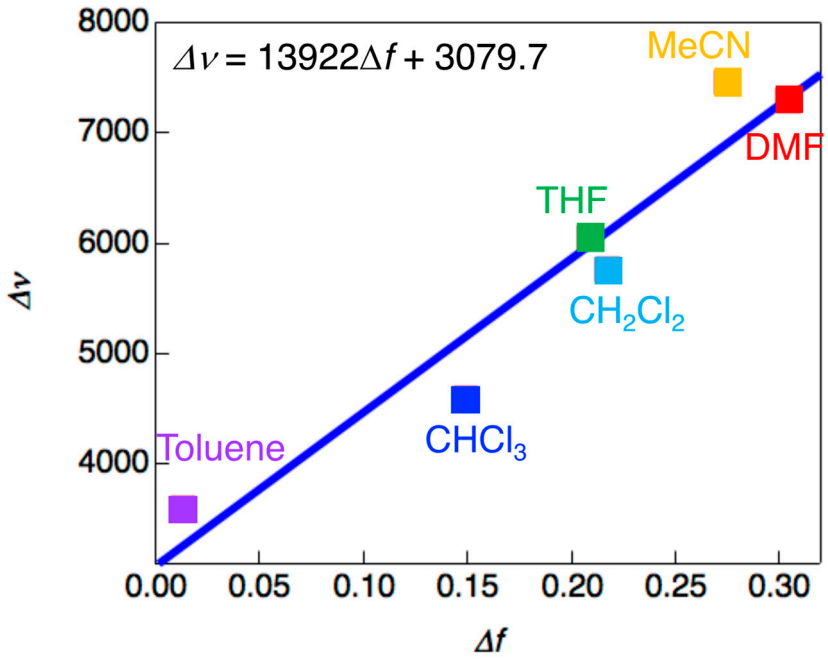

Figure S24. Lippert-Mataga plot of *S*-**2b**.

7. PL behavior in crystal

For excitation and PL measurements, crystalline powder samples were placed between two quartz glass plates, and the samples were placed above a quartz Petri dish and characterized using a calibrated integrating sphere for measurements of PL behavior and PLQY in the crystalline state using a C11347-01 absolute PLQY measurement system (Hamamatsu Photonics KK, Hamamatsu, Japan).

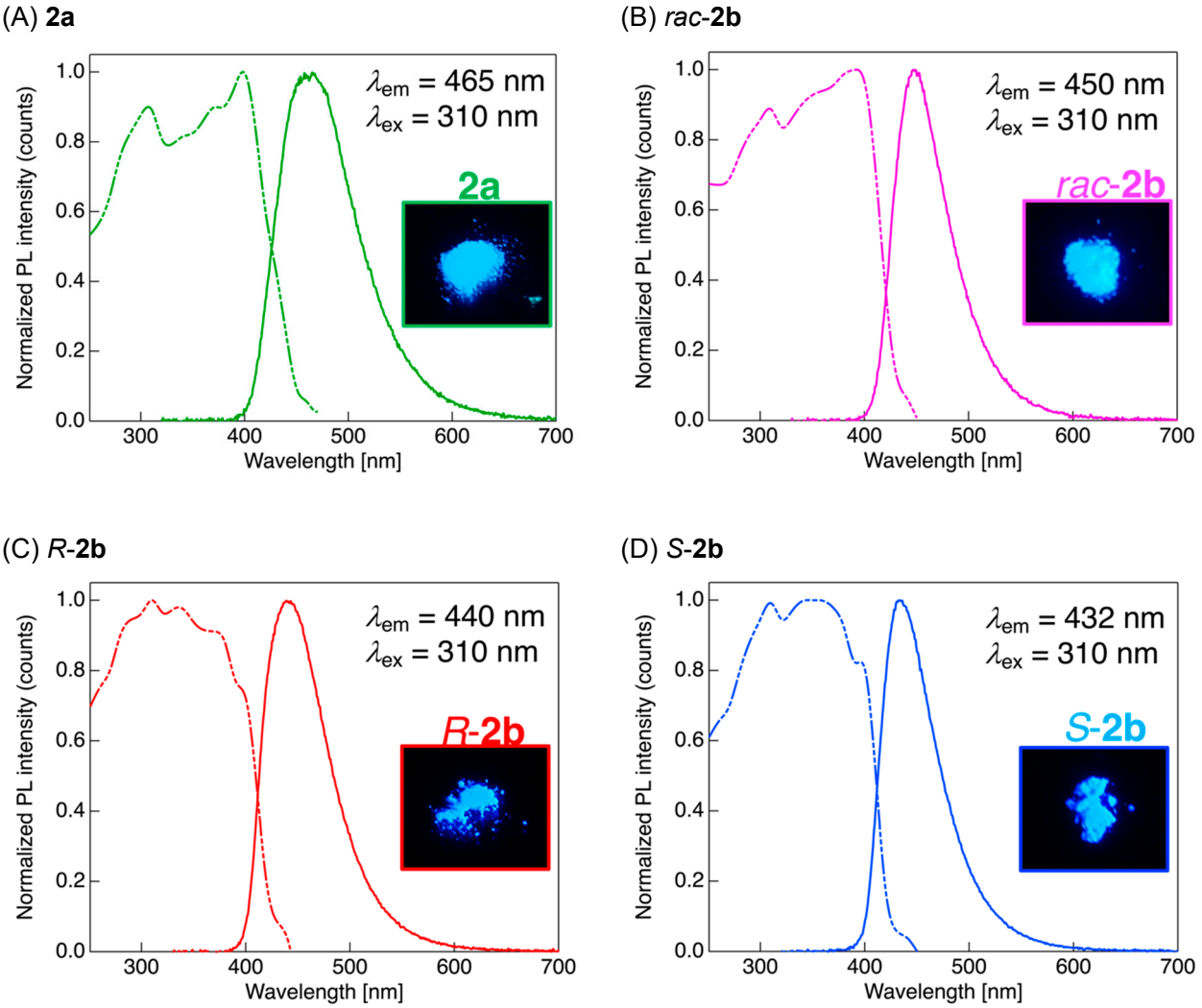

Figure S24. Excitation (dotted line) and PL spectra (solid line) of (A) **2a**, (B) *rac*-**2b**, (C) *R*-**2b**, and (D) *S*-**2b** in crystal. Inset: Photographs of these solutions under UV irradiation (λ_{ex} = 365 nm).

8. PL Behavior in LC phase

For PL measurements in LC phases, samples were prepared by flash-freezing through dipping into a liquid N_2 bath after the thermal phase transition to the LC phase, which allowed us to probe PL behavior at 25 °C while preserving the molecular aggregates in the LC phase. The obtained LC powder was placed between two quartz glass plates. For measurements of PLQY in the crystalline state, samples were placed above a quartz Petri dish and characterized using a calibrated integrating sphere.

(A) **2a** (B) *rac*-**2b**

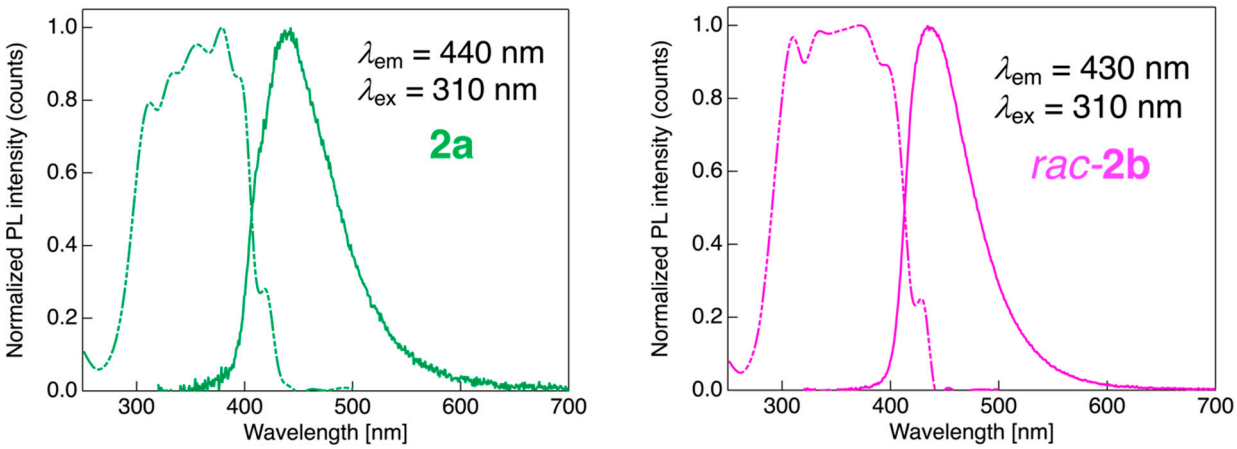

(C) *R*-**2b** (D) *S*-**2b**

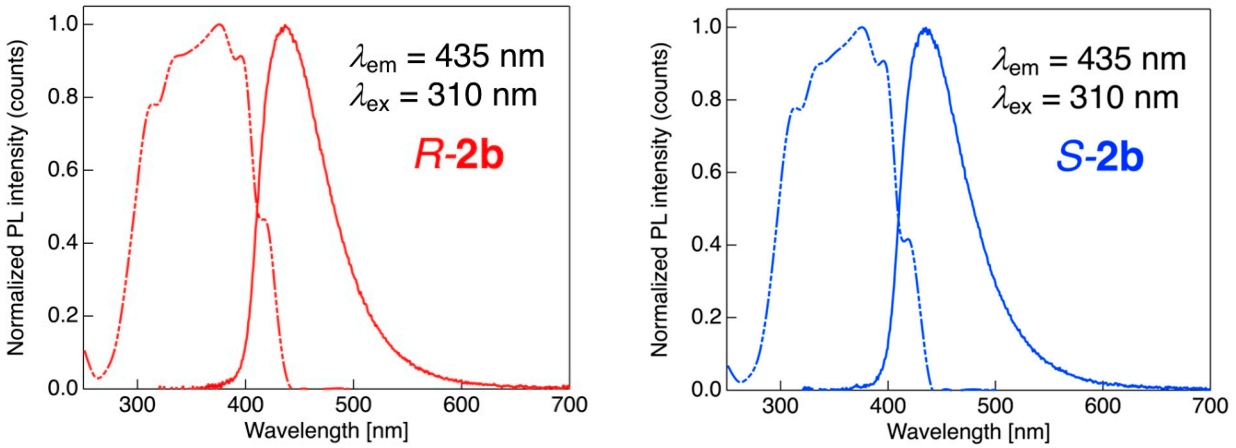

Figure S25: Excitation (dotted line) and PL spectra (solid line) of (A) **2a**, (B) *rac*-**2b**, (C) *R*-**2b**, and (D) *S*-**2b** in crystal.